23
Static electricity

23.1 Introduction

Some of the effects of static electricity were described by Thales in about 600 BC, and the first understanding of the nature of electricity came from the study of the phenomenon of static electricity in the 18th century. After the discovery of current electricity, however, the study of static electricity, with all its experimental difficulties, was neglected, but the increasing amount of trouble in industry that is due to static, resulting from the introduction of new materials, particularly synthetic fibres, led to a revived interest in it [1–3]. Holme *et al*. [4] have published a more recent review. Through its effects, static causes a variety of troubles in textile materials and processing.

Similar charges repel one another. This causes difficulty in handling materials. The filaments in a charged warp will bow out away from one another. There will be 'ballooning' of a bundle of slivers. Cloth will not fold down neatly upon itself when it comes off a finishing machine and so on. Unlike charges attract one another. This has caused difficulty in the opening of parachutes. It will also cause two garments, oppositely charged, to stick to one another, and in movement one garment may ride up on the other and cause embarrassment to the wearer. Another consequence is the attraction to a charged material of oppositely charged particles of dirt and dust from the atmosphere (Fig. 23.1). After 15 days, the soiling of a cotton fabric held at +1.2 kV was over twice as severe as at 0 kV. At –12 kV it was 13 times worse, but at +12 kV it was 19 times worse owing to the preponderance of negatively charged dirt particles in the atmosphere [5]. This fine dirt adheres so firmly that it is difficult to remove and causes serious soiling. When this occurs on the portion of cloth in a loom that is left exposed overnight, it is known as 'fog-marking'. The effects of attraction and repulsion were described by Robert Symmer in 1759, who used to wear two pairs of stockings, white worsted for comfort and black silk for appearance: on separating the stockings: 'the repulsion of those of the same colour, and the attraction of those of different colour, throws them into an agitation that is not unentertaining'.

Charged bodies are attracted to uncharged bodies. Consequently, fibres will stick to earthed parts of machines; this happens particularly in carding. When a charged yarn is passing through a guide, the extra-normal force due to this attraction may notably increase the friction. Another consequence is that uncharged particles in the atmosphere will be attracted to a charged material.

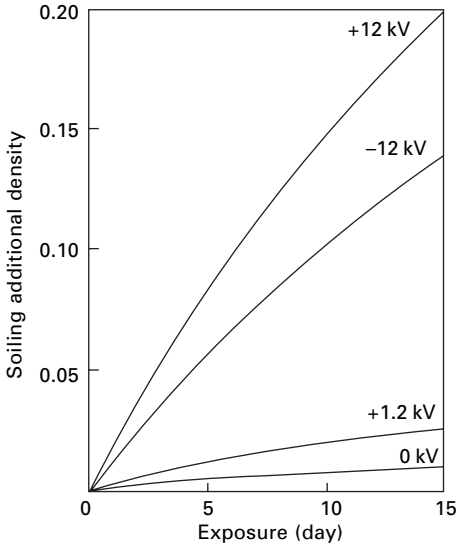

23.1 Effect of potential on soiling of cotton fabric. After Rees [5].

When high enough fields occur, discharge in air will take place with accompanying sparks. This is easily noticeable on taking off charged clothing. The noise of the discharge may be a nuisance in some special cases, for example in the fur hoods worn in arctic conditions. There is also a risk of fire or explosion owing to the sparks. This is a danger in the textile industry only in exceptional circumstances, but sparks from clothing are a source of danger where inflammable vapours are present, as in the operating theatres of hospitals. Shocks will be given to people coming into contact with static charges. These are only serious where a large insulated conductor (for example, a machine on an insulating floor) has become charged up. The remedy is to earth the machine. More commonly, individuals act as condensers with a large capacity. Walking on a carpet or sliding off a car seat can lead to accumulation of a large charge. On touching metal, a door handle or whatever, the discharge gives a nasty shock.

As discussed below, the limiting condition for high static charges, and hence the susceptibility to troubles in use, has been shown to depend on the resistance of the material. Low-resistance materials such as cotton and viscose rayon will rarely give static troubles; higher-resistance materials such as wool, silk and acetate will give trouble more often; and the very high-resistance synthetic fibres will give most trouble. The speed of the process is also important: thus, to avoid fog-marking in weaving, dissipation in 10 minutes, needing a total current of 0.003 μA, is adequate, but, to avoid trouble in carding, dissipation must take place in 0.1 s, which needs 0.07 μA; to avoid trouble in warping, it must take place in 0.01 s, which needs 5 μA.

Methods of getting rid of static charges depend upon increasing the leakage by lowering the resistance of either the material or the air, or by providing a conducting liquid at the separation. The resistance of the material may be lowered by raising the humidity or by moistening it. The resistance of the air may be lowered by ionising it,

either by using a high-voltage static eliminator or by the presence of a radioactive material. Safe concentrations of the latter are only sufficient to cause a slow discharge. The use of electrostatic eliminators in the textile industry has been described by Henry [6]. The use of anti-static agents is discussed by Sagar [7], Götze *et al*. [8] and Holme *et al*. [4]. Unfortunately, the hygroscopic salts that are the most effective anti-static agents are usually unsuitable for other reasons.

23.2 Measurement of static

The methodology can be illustrated by methods used in the earlier studies of textile charging. The principles remain the same, but advances in electronics have changed the devices used in electrical measurements [9]. The amount of static present should be expressed by the magnitude of the charge on the material. This may be measured by the use of a Faraday cylinder. Figure 23.2 shows the apparatus used by Keggin *et al.* [10] to measure the charge on card sliver after carding. The charged material in the cylinder induces an equal opposite charge on the inside of the cylinder (since there can be no net charge inside a closed conductor), and this leaves an equal charge, of the same sign as that on the material, to be shared between the outside of the cylinder and a condenser, which give a total capacitance C. The potential V is measured by a voltmeter and the charge Q can be calculated from the usual expression $Q = CV$.

When the specimen cannot be surrounded, even approximately, by a conductor, the potential to which a neighbouring conductor, the 'probe' electrode, comes may be used as a measure of the charge on the specimen. Unless the geometry is simple enough for the induction coefficients to be calculated, this can give only an arbitrary value. However, when the position, size, shape and charge distribution of the specimen remain constant, it is a useful method for obtaining relative values under different conditions. Some authors have replaced the specimen by a conductor of the same size and shape and, by raising this to known potentials, have obtained a calibration for what they refer to as 'the potential of the specimen'. It is, however, meaningless to

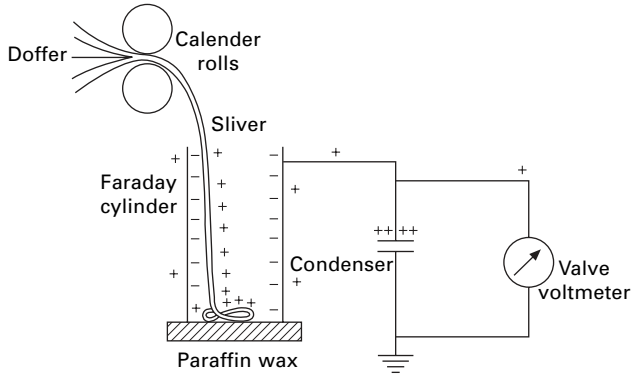

23.2 Measurement of charge by means of a Faraday cylinder. After Keggin *et al*. [10].

talk about the potential of an insulator, since only conductors come to an equal potential at all points.

The potential of the probe electrode may be measured either with a d.c. electrometer or by converting it into an alternating potential. Hayek and Chromey's method [11] (Fig. 23.3(a)), illustrates the latter technique. When the specimen, which has been charged by contact with the paddle, passes the probe electrode, an impulse is transmitted to the measuring circuit. The reading of the detector gives an arbitrary measure of the charge on the specimen. Since the input acts as a resistance/capacity differentiating circuit (Fig. 23.3(b)), it is important that the speed of the drum should be constant.

Another method of obtaining the charge on a specimen, which has been used by Medley [12] and by Gonsalves and van Dongeren [13], is to measure the charge remaining on the conductor from which the specimen is separated. This is illustrated in Fig. 23.4. The potential difference between the rod and earth is indicated on the electrometer, *V*. From a knowledge of the total capacity to earth, the charge left on the rod and the condenser can be calculated. It will be equal and opposite to the charge on the material, provided that no leakage has occurred to other points. If the capacity to earth is large, the rod will remain close to earth-potential but measurable during a test.

The use of electrostatic field meters and voltmeters to measure surface charge distributions is discussed by Seaver [14] and Durkin [15]. Ellison [16] describes a robotic method.

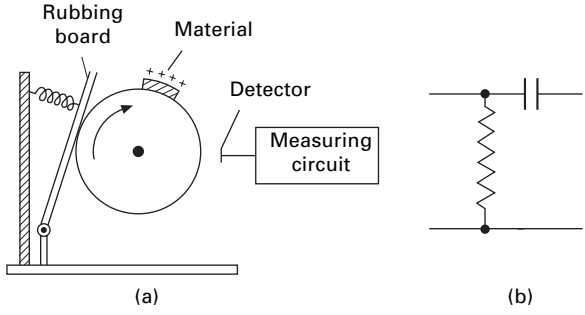

23.3 (a) Intermittent detection by probe electrode. After Hayek and Chromey [11]. (b) Effective input circuit.

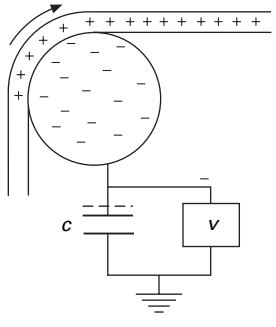

23.4 Measurement of charge remaining on conductor.

23.3 Results

23.3.1 Formation of charge

It was once thought that the conditions necessary for charges to appear were a difference between the nature of the surfaces and rubbing between them. It is now clear that either of these conditions by itself is sufficient. The mere separation of two unlike surfaces has been shown to result in a separation of charge, and Henry [17] and others have shown that the asymmetric rubbing of two identical surfaces results in a transfer of charge.

A familiar idea is that of an electrostatic series, in which materials can be arranged in an order such that, on the separation of any two materials, the higher on the list will be positively charged and the lower negatively charged. However, many workers have produced series that are inconsistent with one another, or have found it impossible to produce self-consistent lists. Henry [17] has shown that, provided that care is taken to minimise non-equilibrium effects due to friction, a series of ten materials could be placed in order with no significant inconsistencies. If the equilibrium charge separations at contact could be measured, not only should they be self-consistent in sign, but the magnitude of the charges should also be additively related to one another. Leakage usually prevents the testing of such a relation, but Harper [18] has shown that it holds for a number of metals. Hersh and Montgomery [19] also found a correlation of the magnitude of the charge generated when metals were rubbed on insulators with the work function[1] of the material and the position of the insulator in the series. Arridge [20] confirmed the correlation with the work function of the metal in experiments on nylon.

Table 23.1 gives the series found in three investigations. Polyamides and wool, which both contain —CO·NH— groups, are at the positive end; cellulose, acrylics and similar materials are in the middle; and the more inert polymers are at the negative end. Cohen [23] suggested that, on the separation of two materials, the one with the high permittivity would become positive; this rule is not of universal validity but may apply to a limited class of materials.

Reversals of the signs of charges owing to very slight (and sometimes undetected) changes of conditions have often been reported. These reversals must be associated with a change in the mechanism of charge transfer. Gonsalves and van Dongeren [13] frequently found a change from positive to negative, as shown later in Fig. 23.9(B)), on an insulator rubbed against a metal as the pressure increased, but they did not find the reverse change.

Martin [24] found that, when a wool fibre was pulled out by the root end from a bundle of wool fibres, all lying in the same direction, it became positively charged, whereas when it was pulled out by the tip end, it became negatively charged.

Owing to slight differences in the surface or the asymmetry in the rubbing, charges may easily be generated by inter fibre contact between apparently identical fibres.

[1]The work function of a metal is the energy needed by an electron in order to free itself from the metal.

Table 23.1 Electrostatic series

	Smith *et al.* [21]	Tsuji and Okada [22]	Hersh and Montgomery [19]
Positive (+)	Wool	Glass	Wooll
	Hercosett wool	Nylon 6.6	Nylon
	Nylon 6.6	Nylon 6	Viscose
	Nylon 6	Wool	Cotton
	Silk	Silk	Silk
	Regenerated cellulose	Viscose	Acetate
	Cotton	*Vinylon* (PVAlc)	*Lucite* (PMMA)
	Poly(vinyl alcohol) (PVA)	*Acrilan* (acrylic)	PVAlc
	Chlorinated wool	Steel	*Dacron* (polyester)
	Cellulose triacetate	Cotton	*Orlon* (acrylic)
	Calcium alginate	*Orlon* (acrylic)	PVC
	Acrylic	Acetate	*Dynel* (VC/AN)
	Cellulose acetate	*Dynel* (VC/AN)	*Velon* (VDC/VC)
	Polytetrafluoroethylene (PTFE)	*Saran* (PVDC)	Polyethylene
	Polyethylene	*Rhovyl* (PVC)	*Teflon* (PTFE)
	Polypropylene	Rubber	
	Poly(ethyleneterephthalate)		
	Poly(1,4-butylene terephthalate)		
	Modacrylic		
Negative (–)	Chlorofibre		

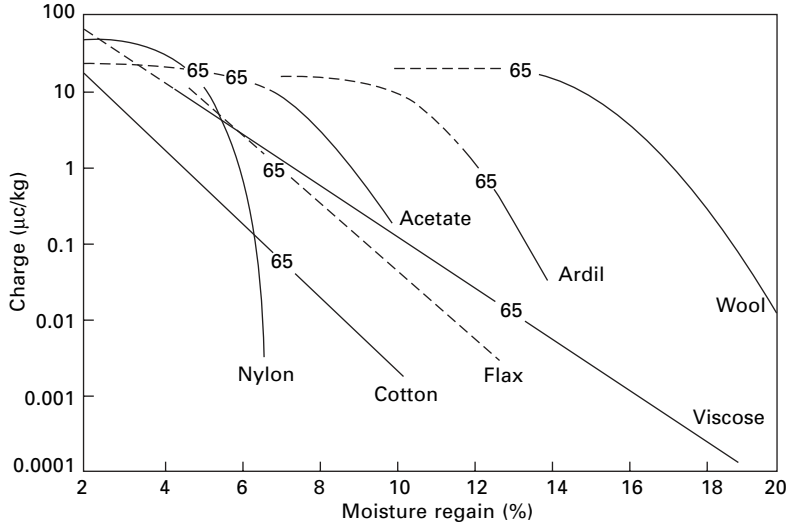

23.5 Charge left on sliver after carding, marking 65% at r.h. level. After Keggin *et al.* [10].

23.3.2 Magnitude of charge

Figure 23.5 shows the charges remaining on the sliver emerging from a card as measured by Keggin *et al.* [10]. It will be seen that at low regains all the materials acquire approximately the same charge. This charge remains constant as the regain

increases until a certain value is reached, and it then drops rapidly for further increases of regain. The points corresponding to 65% r.h. have been marked on the graph, and they illustrate the susceptibility of different fibres to static under the same atmospheric conditions. The amount of static necessary to cause processing difficulties varies from one material to another and is affected by the amount of crimp in the fibre.

Results similar to these have been obtained by Gonsalves and van Dongeren [13] and Medley [12, 25, 26]. The most convenient way of expressing the results is as surface-charge density in microcoulombs per square metre ($\mu C/m^2$). Figure 23.6 shows the charge on nylon film and Fig. 23.7 the charge on single fibres, drawn over platinum rods. It appears that, when the conductance is above a certain value, the charge observed falls rapidly as the conductance increases. A similar result (Fig. 23.8) is obtained when a wool roving that has been coated with a surface-conducting agent emerges from between rollers. The conductance necessary for the rapid drop in charge to start is affected by the speed with which the material is passing through the rollers; the higher the speed, the greater is the conductance necessary. This is shown by the results in Table 23.2. In practice, it is found that the cellulosic fibres are least troubled by static charges; wool and silk are intermediate; and acetate, nylon, polyester, acrylic and other synthetic fibres are most affected. This accords with their electrical resistances as given in Chapter 22.

Medley [26] found that the charge increased with the pressure applied to the rollers, probably owing to an increase in the true area of contact. Gonsalves and van Dongeren [13] found similar results (Fig. 23.9) when the contact pressure for rayon and nylon threads wrapped round a cylinder was increased by increasing either the pre-tension or the angle of wrap. The unfinished rayon thread is an example of the sign change with pressure mentioned earlier (Section 23.3.1). In his experiments

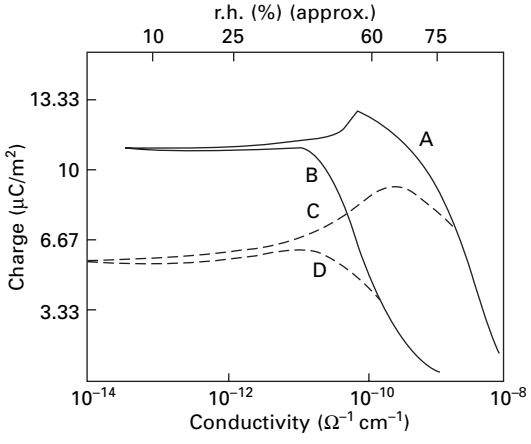

	A	B	C	D
Cylinder diameter (cm)	0.12	0.12	1.25	1.25
Film width (cm)	1	1	2	2
Load (mN)	150	150	50	50
Speed (cm/s)	10	0.5	10	0.5

23.6 Charge developed on nylon film pulled over platinum cylinder [12].

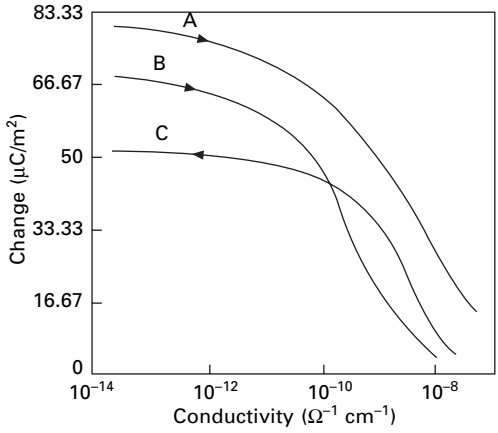

	A	B	C
Material	Nylon	Nylon	Wool
Diameter	20	20	45
Speed (cm/s)	10	0.5	10

23.7 Charge developed on single fibres pulled over 0.1 cm diameter platinum cylinder [12].

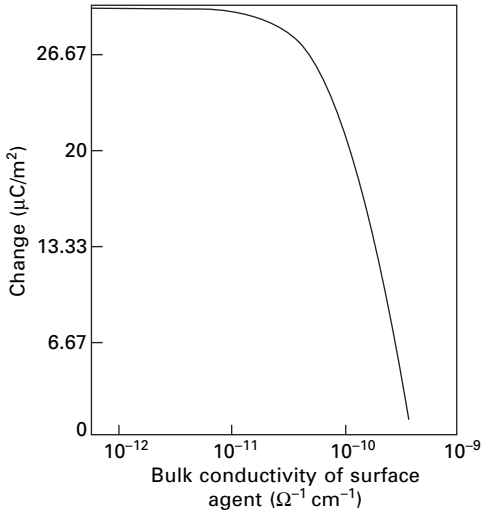

23.8 Electrification of wool roving coated with surface-conducting agent, on pulling through rollers at 10 cm/s [26].

with material emerging from rollers, Medley [26] also measured the charge lost to neighbouring conductors. When charged roving was passed through a small metal loop, its charge was reduced to less than 0.67 μC/m^2: a metal wire held 5 mm below the roving and a metal sheet held 5 cm below it were less effective in discharging the roving.

Lowering the atmospheric pressure reduces the charges that are obtained, as is shown in Fig. 23.10, except at low pressures. In a high vacuum large charges are

Table 23.2 Critical conditions for electrostatic charges (after Medley [25])

(a) Without surface-conducting agents

Material	Rollers	Speed (cm/s)	*Charge halved at:* r.h. (%)	conductance	$\frac{kt}{\varepsilon_0 \upsilon}$ or $\frac{ka}{2\varepsilon_0 \upsilon}$ (see Section 23.5.2) ($\Omega^{-1}\,m^{-1}\,s$)
Woollen taffeta	Steel	5.0	40	$1.2 \times 10^{-12*‡}$	2.8
		2.0	75	$0.4 \times 10^{-12*}$	2.1
		11.0	75	$1.6 \times 10^{-12*}$	1.6
Filter paper	Steel	11.0	40	$1.7 \times 10^{-12*}$	1.8
		15.0	40	$3.4 \times 10^{-12†‡}$	2.0
Wool roving	Cork	11.0	70	$3.6 \times 10^{-12†}$	2.9
a = 0.2 cm		1.25	70	$0.6 \times 10^{-12†}$	4.0

* Ω^{-1} for 1 cm length and breadth equals kt.
† Ω^{-1} for 1 cm length, equals $2\pi a$ (ka).
‡ KC1-treated.

(b) For wool roving with surface-conducting agent. Cork rollers

Aerosol *OT* in combing oil (%)	Bulk conductivity of agent ($\Omega^{-1}\,cm^{-1}$)	Speed at which charge reduced to 12 μC/m^2 (cm/s)
0	2×10^{-12}	Unobtainable
1	1×10^{-10}	3
3	2.5×10^{-10}	10

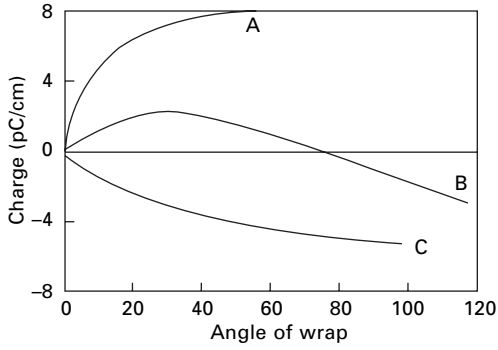

23.9 Effect of wrap on charge on yarn rubbed over steel rod [13]: A, finished rayon; B unfinished rayon; C nylon (approximately 20% r.h.).

obtained. Medley [25] found that, when the air was saturated with carbon tetrachloride, the charge on nylon film increased by 50%. On the other hand, ionising the air reduces the charges that can be obtained.

The maximum charge densities obtained by Medley were about 30 μC/m^2 on films, cloth, and roving and about 160 μC/m^2 on single fibres. Other workers have also found limiting values of about this amount. However, by an ingenious technique,

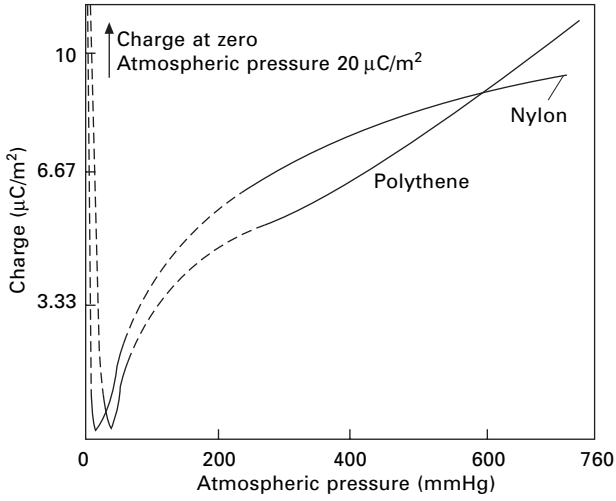

23.10 Effect of atmospheric pressure on charge left on films pulled over platinum wire [12].

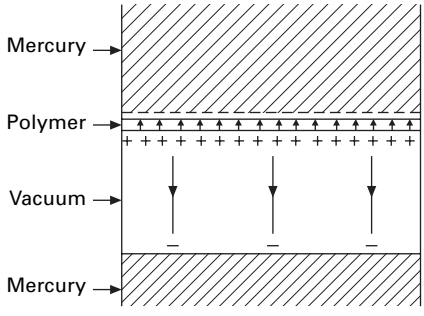

23.11 Charge distribution after separation of mercury from lower surface of polymer.

designed to reduce leakage, Medley [27] was able to obtain much higher values. He separated mercury from a thin layer of polymer, which had another layer of mercury on its opposite side. The whole experiment was carried out in a vacuum. After separation, the charge distribution and electric field will be as shown in Fig. 23.11. The almost equal charge induced on the adjacent layer of mercury after separation can be measured by the usual arrangement of an electrometer and condenser. As soon as the separation has become large compared with the thickness of the polymer, the field in the vacuum will be very small, so that leakage will be negligible. Leakage is possible when the separation is still small, but, under these conditions, the dielectric strength is greater and the insulation is very good. The larger the capacity of the polymer film, the smaller is the chance of leakage. Figure 23.12 shows the results of the experiments. Values of up to 1500 $\mu C/m^2$ were obtained, and it appears that higher values still are possible. If an external electric field is applied, there will be a charge transfer due to the field superimposed on the charge transfer due to the

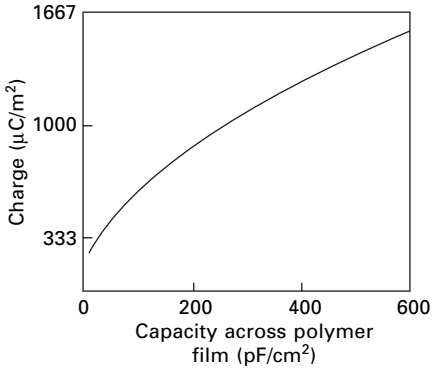

23.12 Charge left after separating polymer film from zinc amalgam [27].

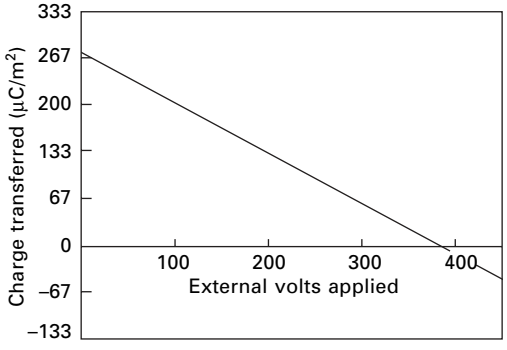

23.13 Effect of applied field on electrification of a nylon film [27].

difference in the two surfaces. According to the direction of the field, this may increase or reduce the charge transfer, and, if large enough, it can even reverse it (Fig. 23.13).

23.3.3 Anti-static treatments

The presence of oil on the surface will influence the charge obtained, as is shown in Table 23.3. Insulating oils may increase the charge, but conducting oils will decrease it. Table 23.4 gives some practical results for various types of anti-static agent. Values for the best and worst material of each type are included. For continued efficacy, finishes must not be lost by washing or wear.

Permanent anti-static behaviour is achieved by the use of conducting fibres. Fibres with moderate conductivity can be used instead of regular fibres in a product, but it is more common to use more highly conducting fibres in small quantities in a blend with other fibres. The inclusion of carbon black to give a conducting path, provided the particles are close enough together, was referred to in Section 22.4.3. However, this has the disadvantage of making the material black. Conductivity can be increased by incorporating hydrophilic groups by copolymerisation or by co-extrusion with a

Table 23.3 Effect of insulating and conducting oil [12]

Insulating oil – liquid paraffin Cowtail fibre – 140 μm diameter Platinum cylinder – 0.123 cm diameter				Conducting oil (180 μm fibre)		
Load on fibre (MPa)	Rubbing	Charge ($\mu C/m^2$) on:		Conductivity of oil ($\Omega^{-1}\,cm^{-1}$)	Rubbing speed (cm/s)	Charge (arbitrary units)
		clean fibre	oiled fibre			
0	Single	0	0	7.5×10^{-13}	5	28
1	Single	13	17	3×10^{-11}	5	8.4
5	Single	25	47	6×10^{-11}	5	1.8
0	Continued	0	0	7.5×10^{-13}	10	30
1	Continued	32	72	3×10^{-11}	10	15
5	Continued	47	94	6×10^{-11}	10	6.8

Table 23.4 Effect of various classes of anti-static agent [8]

Material treated with	Static charge (arbitrary units) 50% r.h.; winding at 180 m/min		
	Viscose rayon	Acetate	Nylon
(Untreated)	47	60	128
Hygroscopic salts	17–38	0–29	3–19
Polyalcohols	45–46	22–33	92–98
Soaps	35–48	21–32	64–88
Sulphonated fatty compounds	34–52	16–32	32–85
Non-ionogenic products	31–42	18–43	22–78
Cation-active products	32–54	15–38	31–62

conducting polymer. For example *DuPont* incorporated streams of colourless polymer in their anti-static nylon carpet fibres. Metal fibres, e.g *Bekinox* stainless steel fibres, which are made with diameters from 2 to 22 μm, have high conductivity.

A more extensive discussion of the chemistry, effectiveness and durability of the many ways of reducing static is given by Holme *et al*. [4].

23.4 Generation of charge

Henry [28–30] has summarised the chief hypotheses that have been put forward to explain the separation of charge on materials in contact. None of them has been convincingly proved to be the sole mechanism, and he suggests that probably all the mechanisms operate to varying degrees in different cases. Whenever two surfaces are brought into contact, it is likely that some charge transfer across the surface will occur, but the conditions that affect it need to be worked out. Some of the charge transfer will result from the equilibrium distribution of charged particles between the surfaces and some from kinetic effects due to such transient influences as temperature differences. It may be noted that the highest observed charges (1500 $\mu C/m^2$) would be explained by the transfer of relatively few charges: one electronic charge for every

100 nm^2 (10 nm × 10 nm) would be sufficient. This area would cover many hundreds of atoms.

It is therefore a general rule that, unless the electrical states of two materials are extremely well balanced, there will be a large transfer of charge when their surfaces are brought in contact. The theories discussed below as a justification for this generalisation suggest that charge densities of 10^5 μC/m^2 would be commonplace. These values are far in excess of what is observed in practice, where the charge levels are reduced by leakage after separation of the surfaces. It is very difficult to get two surfaces in perfect electrical balance, and, even if it were achieved, the balance would be very easily disturbed by the slightest change of conditions. Charge generation is therefore very difficult to avoid.

There is one possible exception to this rule. Charge separation does require the *movement* of some free charges (electrons or ions). If, in an extremely good insulator, there are no mobile ions or electrons at all, then the charge separation will not occur, although charges may be deposited on the material. This may explain why polypropylene fibres appear to cause fewer static problems than some other synthetic fibres, despite their very high resistance.

The various possible mechanisms of charge transfer, which were discussed in more detail in previous editions of this book, are as follows:

1. Difference in contact potential between two metals in contact, due to difference in energy levels of electrons.
2. Difference in energy levels involving insulators, complicated by the presence of forbidden bands and extra levels on the surface [31, 32].
3. Activation by pressure making lower energy levels accessible and leading to charge reversal from positive to negative [32], as in Fig. 23.9. The reverse is not observed.
4. Presence of mobile cations on an acidic surface or mobile anions on a basic surface. Medley [33] observed this effect due to salt linkages, R—$COO^{-+}H_3N$, in keratin. On treatment with HCl, this changes to R—COOH $Cl^{-+}H_3N$, giving a mobile Cl^- ion. Treatment with NaOH gives R—$COO^{-+}Na$ H_2N + H_2O, with a mobile Na^+ ion. On separating keratin from filter paper, the charge reversed depending on the treatment.
5. Asymmetric rubbing leads to thermal gradient, due to action being distributed along a length of one surface and at one place on the other. Charged mobile particles will move from hot to cold.
6. Symmetrical rubbing may give local asymmetry due to high spots on the surfaces. This is illustrated by a distribution of opposite charges over the surface of a polyethylene sheet when it is rubbed against another sheet [17]. In another example, different charges are found when a fibre is drawn from a lock of wool with or against the scales [24].
7. A double layer on a surface may be rubbed off on to another surface.
8. Piezo-electric polarisation due to pressure may lead to charge separation. In wool, pressure leads to the root end becoming negative and the tip end positive, which Martin [24] suggests may be the cause of the charging of wool withdrawn from a lock.

9. A pyro-electric effect at hot spots. Martin [24] found that wool became negatively charged at the root end on immersion in liquid air.

Henry [28–30] combines the first three mechanisms in an instructive example, which is simplified in that it considers the transfer of only one type of particle and uses classical mechanics, which will not be valid if electrons are involved. For electrons, quantum mechanics should be used. A charged particle between two surfaces is repelled by short-range forces when it is very near one of the surfaces, but it is attracted to the surface by the induced 'image' electrostatic forces when it is at a greater distance away. The combination of these forces results in the potential energy diagram shown in Fig. 23.14(a).

We consider unit area with n_1 ions on the first surface, which is at a temperature T_1, and n_2 ions on the second surface at a temperature T_2. The number of ions crossing the barrier $(V_m - V_1)$ per unit area per unit time will be proportional to $n_1 T_1^{\lambda} \exp[-(V_m - V_1)/k\,T_1]$. The index λ varies according to the particular theory in statistical mechanics employed and need not be specified here. Quantum mechanics would give a less simple energy term, owing to the possibility of the passage of particles through the barrier by means of the tunnel effect. There will be a similar loss of ions from the second surface over the barrier $(V_m - V_2)$. The difference in transfer rates will cause a separation of charge and will give rise to an electrostatic field, which will change the potential energy diagram. This will continue until the electrostatic field is such as to equalise the rates of transfer from each side. If E_1 and E_2 are then the electrostatic potentials at the surfaces, and E_m that at the position of maximum total energy, and if V_m is also now taken at this position (Fig. 23.14(b)) the rate changes to $n_1 T_1^{\lambda} \exp\{[-(V_m - V_1) + e\,(E_m - E_1)]/k\,T_1\}$, where e is the charge on the ion. There is an analogous expression for the reverse direction. Equilibrium will occur when the two rates are equal. An external electric field F, which also changes the height of the barrier, can be added to the model.

The analysis continues so as to predict the charge densities $\pm Q$ on surfaces separated by a distance D. We write $(V_1 - V_2) = (W_2 - W_1) = \Delta W$, where W_1 and W_2 are the amounts of work needed to remove the type of ion concerned from the surfaces into a vacuum and $V + eE = U$. The value of Q is given by:

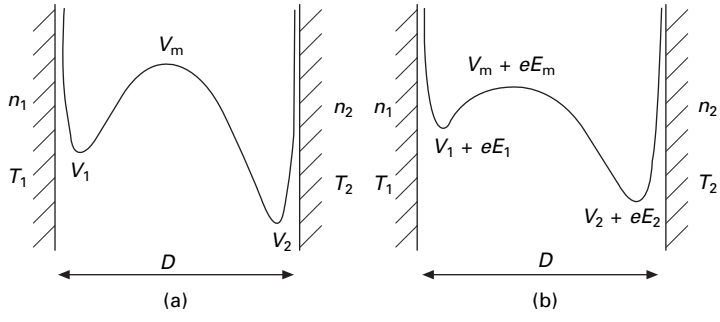

23.14 Potential energy of charged particles between two surfaces: (a) in absence of electrostatic field; (b) at equilibrium, with electrostatic field.

$$4\pi eDQ = -\Delta W + kT\log_e\left(\frac{n_2}{n_1}\right) + \Delta T/T\left(\lambda kT + U_m - \frac{U_1 + U_2}{2}\right) - eDF \tag{23.1}$$

In this expression, $-\Delta W$ represents the difference in energy levels, that is, the contact potential of mechanisms 1 and 2. The second term represents the effect of the different concentrations, n_1 and n_2, on the two surfaces, that is, mechanism 3. The third term gives the effect of the difference in temperature, ΔT, between the two surfaces, that is, mechanisms 4 and 5. Of this term, the first part within the brackets is an effect similar to thermal diffusion, while the other terms derive from the potential energy 'hump' that has to be overcome. The final term in the expression represents the effect of an external field, which gives rise to an additional charge density sufficient to produce an equal and opposite field. This example illustrates how the various effects combine together. The other mechanisms listed may also come in as additional effects.

Charges as great as those which would be predicted on these theories, amounting to more than $10^5\,\mu C/m^2$, are rarely observed in practice. Leakage, through either the air or the material, usually occurs and limits the observable charge. This fact makes experimental investigation of charge generation difficult. Leakage also explains the absence of a difference in magnitude of the charge obtained from the distance apart in the electrostatic series and the apparent abruptness with which reversals of charge occur. Whereas the original charge separation may vary continuously from a high positive to a high negative value as conditions change, the observed charge will drop in a step from a constant positive value to a constant negative value, as is illustrated in Fig. 23.15.

23.5 Leakage of charge

23.5.1 Leakage in air

As discussed above, the inherent magnitude of charge separation is much greater than observed charges, unless the two surfaces are almost perfectly balanced. The

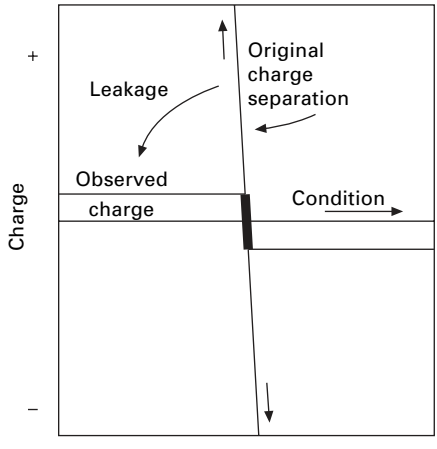

23.15 Original and observed charge separation.

observed charges depend primarily on the extent to which the charge can leak away and this can happen in a variety of ways.

When the material is completely non-conducting, leakage through the air is the only factor that limits the static charge and it is an important factor in materials with low conductivity. The breakdown potential of air at atmospheric pressure is 30 kV/cm, and this means that the maximum charge which can exist on a plane surface is about 30 μC/m^2. For a sheet with two surfaces, 60 μC/m^2 should be possible, but, in fact, uneven charging and irregularity of the surface usually prevent more than half this amount from being observed. If the material is passing over a rod, the leakage will occur through the air back to the rod, as shown in Fig. 23.16. The presence of other neighbouring conductors may cause a concentration of lines of force, as shown in Fig. 23.17, resulting in a discharge to the conductor and leaving a smaller charge density on the material. This has been found by Medley [26], who has discussed the conditions necessary to cause the greatest discharge. The field strength will also be influenced by the shape of the specimen and by the presence of neighbouring charges. For example, single fibres can support high surface charges (about 150 μC/m^2) owing to the rapid decrease of field strength as the lines of force diverge from the fibre. Where fibres are grouped together, as in a roving, however, such high fibre-surface charges are not possible, since the combined field at the outside of the roving would then exceed the dielectric strength of the air.

It is the limitation of charge by conduction in air that results in the constant portion of the curves of charge versus relative humidity or conductance of the material. There may even be a slight increase (as in Fig. 23.6) since, under some conditions, the dielectric strength of air is greater at a higher humidity. Near atmospheric pressure,

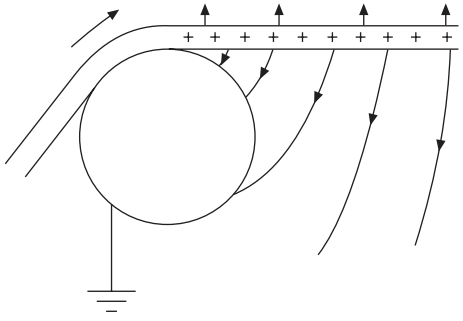

23.16 Electrostatic field causing leakage through air back to rod.

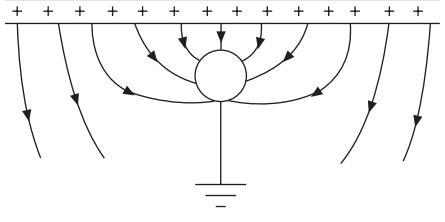

23.17 Concentration of lines of force due to neighbouring conductor.

the dielectric strength of air decreases as the pressure drops, which results in a decrease in the observed charge (Fig. 23.10), but in a good vacuum the dielectric strength is high and the observed charges are high. The particular advantage of Medley's technique [27] of backing a thin film of polymer with mercury (see Section 23.3.2) is that the field due to the charge decreases rapidly as the separation of the surfaces increases. In a sufficiently narrow gap, the ions present cannot accelerate enough for ion multiplication by collision to occur; consequently, the breakdown strength increases. At atmospheric pressure, this increase in dielectric strength occurs when the gap is reduced to a few microns, but at low pressures it occurs at greater thicknesses. Thus in the initial stages of the separation, while the field is high, the dielectric strength is also high.

Anything that increases the dielectric strength of the atmosphere, such as saturation with carbon tetrachloride, results in an increase of the limiting charge that can be obtained. Conversely, lowering the resistance of the air by ionising it reduces the limiting charge. Static eliminators, which apply a high voltage to metal points, work on this principle. Alternatively, radioactive material will ionise the air.

To make a complete quantitative analysis of the charge left on the separated material after leakage has occurred, one would need to work out the distribution of electric field in the system and the currents that would flow as a result of the electric field. Working out the field is a complex problem owing to the disturbing influence of dielectrics and conductors in the system. The mathematical difficulty is further increased when current flows, since this alters the charge distribution and consequently alters the electric field producing the current.

The electric fields are determined not only by the charge on the insulator but by image charges in the neighbouring conductor. Medley [12], neglecting the effect of the dielectric constant of the material and using an approximate image system, worked out the field due to an approximately uniform charge distribution on a thin sheet of material separated from a conducting cylinder and parallel to a conducting plane. It can then be seen where the dielectric strength of the air is exceeded. By analysis or successive approximation, a modified charge distribution, taking account of the leakage in air, can be worked out.

In practice, an approximate value can be obtained by assuming that just beyond the point of separation, or just beyond a conductor whose influence is being considered, the charge density is reduced to a uniform value, σ_a, giving a field equal to the dielectric strength of air, E_{crit}. For a plane surface, by the application of Gauss's theorem, this gives:

$$\sigma_a = \frac{2\varepsilon E_{crit} \cos\theta}{\alpha} \tag{23.2}$$

where ε = permittivity of air ≈ permittivity of vacuum, α = ratio of the normal flux density to the average normal flux density on both sides of the surface, and θ = angle between lines of force and the normal to the surface.

High values of θ will be dominant, giving cos = 1 at 90°. The ratio α will be limited to values between 0 and 2, and, unless there are marked disturbing effects due to dielectrics or conductors near the charged surface, it will be approximately equal

to 1. Thus $(\cos\theta/\alpha) \sim 1$. With $\varepsilon_0 = 8.85$ pF and $E_{crit} \sim 4$ MV/m, this indicates a maximum charge density of the order of 10 μC/m^2 in accord with the usual observations. It will be lower when the electric field is concentrated and higher when special precautions are taken to limit the discharge.

23.5.2 Leakage in the material

As soon as the resistance of the material becomes low enough for appreciable current to flow through it, the observed charge starts to decrease. Since a small increase in humidity causes a large increase in conductance, the curve of charge against relative humidity then drops rapidly, as is shown in Figs 23.6–23.8.

Once again, exact analysis is difficult, but the influence of the material may be illustrated diagrammatically. In a perfect insulator (Fig. 23.18(a)), no current flows through the material and a charge, limited by air leakage, remains on the surface. In a moderate insulator (Fig. 23.18(b)), the charge left after leakage through the air can spread out from the surfaces where it first appears. This gives an electric field acting back along the material, since at a distance the effect of the double layer is negligible.

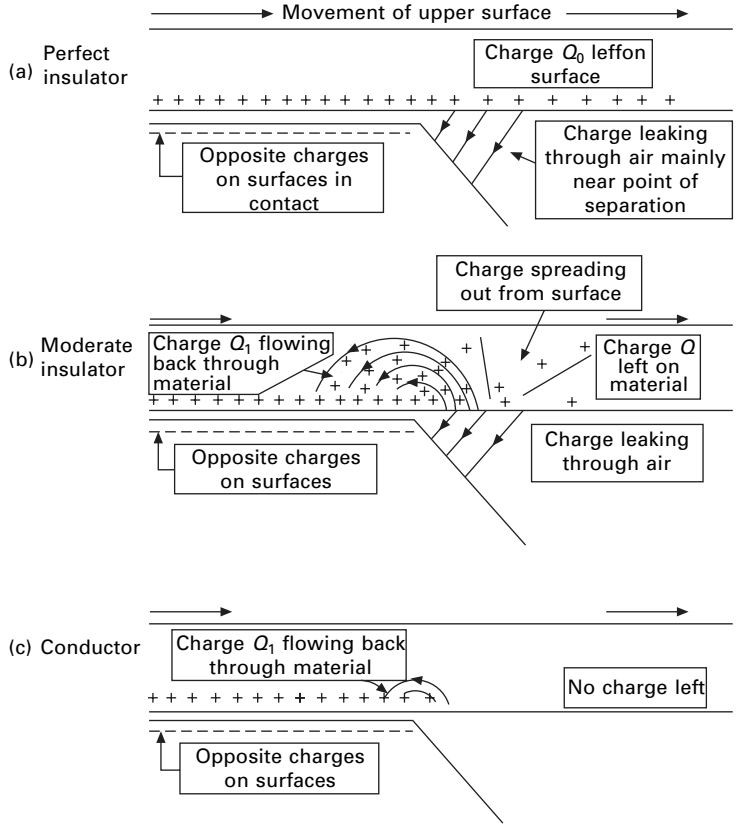

23.18 Leakage of charge in (a) perfect insulator, (b) moderate insulator and (c) conductor.

Some charge will flow back behind the point of separation and become a source of charge for the double layer at the surfaces in contact. In a good conductor (Fig. 23.18(c)), there will be a large backward current and the charge will never get far beyond the point of separation but will, in effect, be circulating near the surfaces in contact, and never penetrating deeply into the material.

The currents will flow in the reverse direction to the movement of the material that is carrying charge forward. Consequently, the greater the speed of the material, the smaller will be the reduction of charge for a given conductance. This means that the higher the speed of a process, the more likely is the occurrence of static charges.

If we consider unit width of material (Fig. 23.19), of thickness t and conductivity k, moving with a velocity v, and having a charge per unit area σ (not necessarily all on the surface), then the rate of transport of charge past a given point owing to the movement of the material is σv. If there is an electric field E, with a component ($E \sin\phi$) in the opposite direction to the motion, the current flowing will be ($E \sin\phi \cdot kt$). The net rate of transfer of charge is therefore ($\sigma v - E \sin \phi \cdot kt$).

In the steady state, this must be equal at all points along the material, and a relation between σ and $E \sin \phi$ is thus established. If σ' is the limiting charge per unit area left on the material at a long distance from the point of separation, we must have:

$$\sigma' v = \sigma v - E \sin \phi \cdot kt \tag{23.3}$$

$$\sigma' = \sigma - E \sin \phi \frac{kt}{v} \tag{23.4}$$

Using this relation, and deriving values of E from the approximate image system, Medley [12] worked out, by successive approximations, the charge distribution in the steady state for material coming off a cylinder of unit diameter. This shows that, owing to the influence of the induced charge on the cylinder, a maximum in the charge on the material occurs some distance beyond the point of separation and thus most of the current will finally reach the cylinder by discharge across the gap, rather than by conduction behind the point of separation. This effect is less marked when the ratio of thickness of material to diameter of cylinder is greater.

We may obtain an approximate expression for σ' in the following way. For surface charge on a dielectric material remote from conductors, the field in the dielectric is ($\sigma/2\ \varepsilon_r\ \varepsilon_0$). We may therefore put $E \sin \phi = \Phi\sigma/2\varepsilon_0$, where it follows from the geometry of Fig. 23.20 that $\Phi = (2 - \alpha) \tan \phi/\varepsilon_r$ and is a dimensionless function

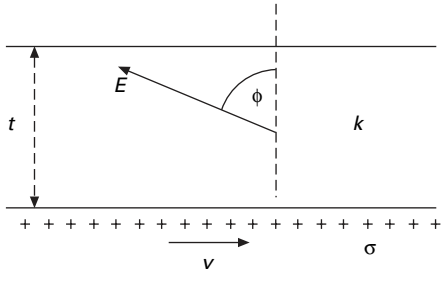

23.19 Field in specimen.

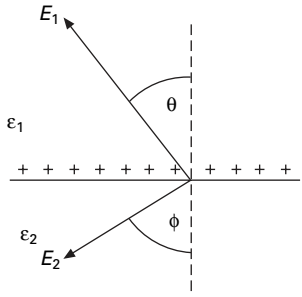

23.20 Effect of surface charge. If σ is the surface density of charge and E_1 and E_2 are electric fields making angles θ and ϕ with the surfaces of two media of permittivity ε_1 and ε_2, then by Gauss's theorem: $\varepsilon_1 E_1 \cos\phi + \varepsilon_2 E_2 \cos\phi = \sigma$. Hence:

$$\phi = \frac{\varepsilon_1 E_1 \cos\theta}{\frac{1}{2}(\varepsilon_1 E_1 \cos\theta + \varepsilon_2 E_2 \cos\phi)} = \frac{2\varepsilon_1 E_1 \cos\theta}{\phi}$$

$$= 2\,\varepsilon_r\,\varepsilon_0\,E_1\cos\theta/\sigma,$$

where ε_r is the relative permittivity of medium 1 and ε_0 is the permittivity of a vacuum.

depending on the relative permittivity and the field distribution in the particular system.

Substituting in equation (23.3), we get:

$$\sigma' = \sigma\left(1 - \frac{\Phi k t}{2\varepsilon_0 v}\right) \tag{23.5}$$

Near the point of separation, σ will drop to the value σ_a, limited by air discharge given by equation (23.2), and we have[2]:

$$\sigma' = \sigma_a\left(1 - \frac{\Phi k t}{2\varepsilon_0 v}\right) = \frac{2\varepsilon_0 E_{crit}\cos\theta}{\alpha}\left(1 - \frac{\Phi k t}{2\varepsilon_0 v}\right) \tag{23.6}$$

It follows from this equation that the charge remaining on the material is a fraction of the maximum value determined for different systems by the value of (kt/v). It can be noted that kt is the conductance (reciprocal of resistance) per unit width per unit length. The charge will drop to half the maximum value when $(kt/\varepsilon_0 v)$ equals $1/\Phi$. Considering that values of (kt/v) cover a range of at least a million to one, the results given in Tables 23.2 and 23.5 support this view and indicate that $1/\Phi$ lies between 1 and 7.

[2]The various expressions quoted here will only be correct in a consistent set of units. In SI units, this means that the conductivity k should be in $\Omega^{-1}\,m^{-1}$, the thickness t in m, and the velocity v in m/s. The permittivity ε_0 is in the usual units (F/m or $kg^{-1}\,m^{-3}\,s^4\,A^2$) and has the value 8.85×10^{-12} F/m. The product (kt/v) will have the units $\Omega^{-1}\,m^{-1}$ s, which also, as should be the case, are equal to $kg^{-1}\,m^{-3}\,s^4\,A^2$. We may note that $kt/2v$ will have the same units if k is expressed in $\Omega^{-1}\,cm^{-1}$ and t in cm, with v in m/s.

Table 23.5 Critical conditions for reduction of charge [12]

$\frac{kt}{\upsilon}$ or $\frac{ka}{2\upsilon}$	Values of fraction of maximum charge for systems below						
(Ω^{-1} m^{-1} s)	A	B	C	D	E	F	G
1.3					0.71	0.56	0.67
1.6	0.91	0.80	0.96	0.91			
6.3	0.45	0.52	0.67	0.65			
12.6	0.30	0.30			0.24	0.25	0.19

System	25 μm Nylon strip on platinum cylinder			
	Width (cm)	Load (mN)	Cylinder diameter (cm)	Speed (cm/s)
A	1	150	0.12	0.5
B	1	150	0.12	10
C	2	50	1.25	0.5
D	2	50	1.25	10

Single fibres, 0.1 cm platinum cylinder

	Material	Diameter (μm)	Speed (cm/s)
E	Nylon	20	0.5
F	Nylon	20	10
G	Wool	45	10

Equation (23.6) will cease to hold when kt/v becomes large, and the expression approaches zero and then becomes negative. The derivation is only valid when the current flow is relatively small.

As ε_r increases, the line of force would tend to concentrate in the dielectric material, which would increase ϕ. So, as a rough approximation, $\tan \phi = \varepsilon_r \tan \theta$, which indicates that $\Phi \approx (2 - \alpha) \tan \theta$. For $\theta = 20°$ and $\alpha = 1$, this would make $1/\Phi$ equal to 2.8, in agreement with the experimental results.

For a cylindrical specimen of radius a, equation (23.5) changes to:

$$\sigma' = \sigma\left(1 - \frac{\Phi k a}{4\varepsilon_0 v}\right) \tag{23.7}$$

23.5.3 An alternative leakage equation

The expression $E \sin \phi = \Phi\sigma/2\varepsilon_0$ above (21.11) is an approximation because the charge causing the electric field E will be not the unreduced value σ but some average of values between σ, near to the point of separation, and σ', at a remote position. This is the source of error in the derivation, which makes the equation invalid for large values of kt/v. If we adopt the other extreme possibility, we put $E \sin \phi = 2\pi\sigma'\Phi$. This leads to:

$$\sigma' = \sigma\left(1 + \frac{\Phi k t}{2\varepsilon_0 v}\right)^{-1} \tag{23.8}$$

A comparison of the predictions of the two equations (23.5) and (23.8) is shown in Fig. 23.21. The actual behaviour should lie between the predictions of the two equations, as indicated by the dotted lines.

23.5.4 The action of a surface coating

It has already been mentioned that, when the material is a good conductor, the leakage does not penetrate deeply into the material. Consequently, a thin permanent conducting layer on the surface of a fibre would reduce static charges, but Medley [12] has pointed out that the action of a surface dressing may be slightly different from this.

A liquid dressing may not separate the two materials but may instead form a wedge-shaped film at the point at which they diverge from one another, as shown in Fig. 23.22. This liquid will act as a leaky dielectric, and dissipation of charge will occur owing to current flow across it. The time constant of a condenser is independent of its size and shape, and the decay of charge is given by the relation $\sigma = \sigma_0 \exp(-tk/\varepsilon)$ where σ_0 is the initial charge density, σ is the charge density at time t, ε is the permittivity of the liquid, and k is its conductivity. If v is the speed of the material and δ the length of the wedge, the time for a given portion of material to pass the liquid is δ/v, and therefore:

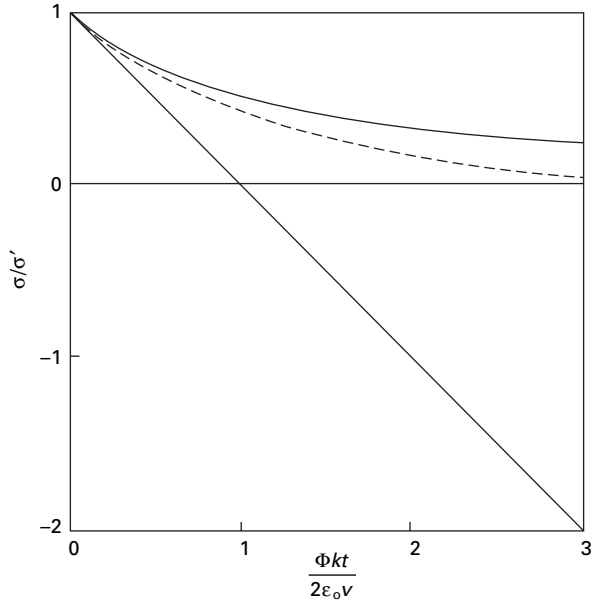

23.21 Comparison of prediction of equations (23.5) and (23.8), with indication (dotted) of likely real relation.

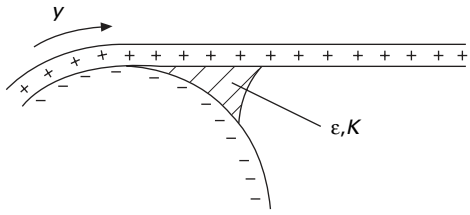

23.22 Wedge-shaped film at point of separation.

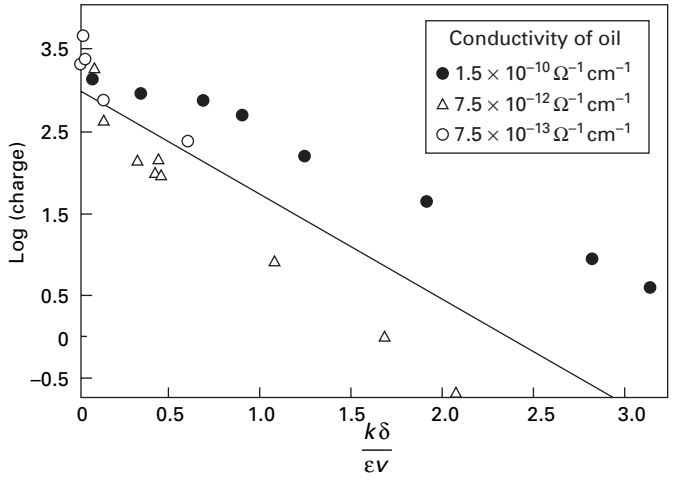

23.23 Reduction of charge on wool fibre due to conducting oils [12]. The line represents equation (23.10). Charge is in arbitrary units.

$$\sigma = \sigma_0 e^{-k\delta/\varepsilon v} \tag{23.9}$$

$$\log_e \frac{\sigma}{\sigma_0} = -\frac{k\delta}{\varepsilon v} \tag{23.10}$$

Figure 23.23 shows an experimental check of this relation for varying rubbing speeds and three different mixtures of liquid paraffin and Lubrol MO.

It will be seen from equation (23.9) that the condition for marked reduction of electrification is $\varepsilon v < k\delta$. It may be noted that the quantity $k\delta/\varepsilon v$, equal to $k\delta/\varepsilon_r\varepsilon_0 v$, is a dimensionless parameter.

It follows from this view of the action of an anti-static agent that it need not be present on the fibres but can be present on the guide or roller in order to give the wedge-shaped film. Medley [12] found that a porous cast-iron roller, impregnated with *Empilan* A (conductivity of $10^{-7}\,\Omega^{-1}\,cm^{-1}$), produced negligible static in worsted drawing, in contrast to the behaviour of an ordinary roller. This procedure does not, of course, meet the need for a permanent anti-static dressing to prevent the troubles due to static in use.

If the liquid is not a conductor, leakage will not occur, and the observed charges may even increase (as in Table 23.3), owing to the greater dielectric strength of the

liquid than that of air. This will reduce discharge in the region near the point of separation where the field is greatest.

Graham [34] has taken a rather different view of the action of anti-static agents. Figures 23.24 and 23.25 show the effect of five liquids on the charge given when nylon is rubbed over brass. He suggests that if it is thick enough, the liquid film prevents the contact potential between the two surfaces from becoming effective and that, if separation then occurs within the film, no charge will result. He associates the more effective action of the liquids with the higher dielectric constants to their greater degree of shielding. For this mechanism to be effective, the liquid film must be reasonably isotropic. With the surface-active agents, Fig. 23.25, the molecules are regularly oriented, and reversals in their effect occur as increasing amounts are applied. The reversals correspond to successive monomolecular layers and will be associated with the surfaces changing from polar to inert groups and vice versa. With triethanolammonium oleate, the regularity breaks down with larger amounts, but it persists to thick layers with potassium oleate.

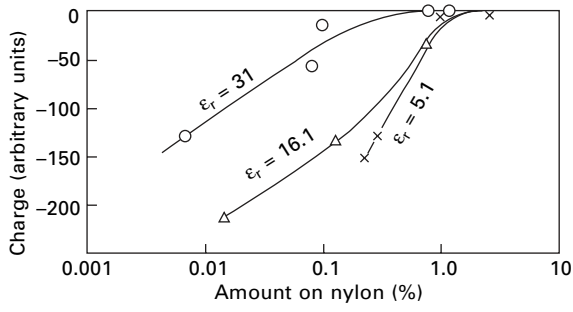

23.24 Effect of relative permittivity ε_r of surface dressing on charge. After Graham [34].

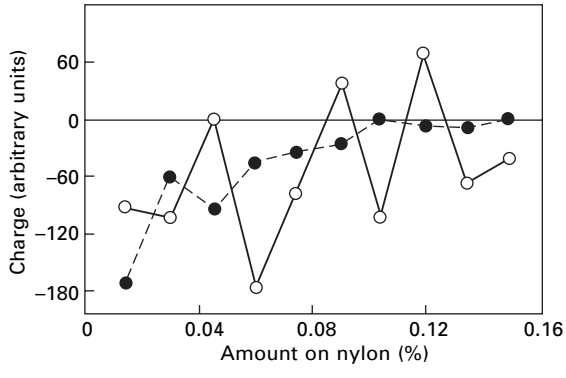

23.25 Effect of surface activity on charge: ○ potassium oleate; ● Dotted line: triethanolammonium oleate. After Graham [34].

23.6 References

1. *Brit. J. Appl. Phys.*, 1953, Supplement No. 2: 'Static Electrification' (report of Conference).
2. *J. Text. Inst.*, 1957, **48**, P4: 'Static Electricity in Textiles' (report of Conference).
3. D. F. Arthur. *J. Text. Inst.*, 1955, **46**, T721 (review of literature).
4. I. Holme, J. E. McIntyre and Z. I. Shen *Textile Progress*, **28**, No. 1, 1998.
5. W. H. Rees. *J. Text. Inst.*, 1954, **45**, P612.
6. P. S. H. Henry. *Brit. J. Appl. Phys.*, 1953, Suppl. No. 2, S78.
7. H. Sagar. *J. Text. Inst.*, 1954, **45**, P206.
8. K. Götze, W. Brasseler and F. Hilgers. *Melliand Textilber.*, 1953, **34**, 141, 220, 349, 451, 548, 658, 768.
9. P. E. Secker and J. N. Chubb. *J. Electrostatics*, 1984, **16**, 1.
10. J. F. Keggin, G. Morris and A. M. Yuill. *J. Text. Inst.*, 1949, **40**, T702.
11. M. Hayek and F. C. Chromey. *Amer. Dyest. Rep.*, 1951, **40**, 164.
12. J. A. Medley. *J. Text. Inst.*, 1954, **45**, T123.
13. V. E. Gonsalves and B. J. van Dongeren. *Text. Res. J.*, 1954, **24**, 1.
14. A. E. Seaver. *J. Electrostatics*, 1995, **35**, 231.
15. W. J. Durkin. *J. Electrostatics*, 1995, **35**, 215.
16. M. S. Ellison. *J. Textile Inst.*, 1991, **82**, 512.
17. P. S. H. Henry. *Brit. J. Appl. Phys.*, 1953, Suppl. No. 2, S31.
18. W. R. Harper. *Proc. Roy. Soc.*, 1951, **A205**, 83.
19. S. P. Hersh and D. J. Montgomery. *Text. Res. J.*, 1955, **25**, 279.
20. R. G. C. Arridge. *Brit. J. Appl. Phys.*, 1967, **18**, 1311.
21. P. A. Smith, G. C. East, R. C. Brown and D. Wade. *J. Electrostatics*, 1988, **21**, 81.
22. W. Tsuji and N. Okada. Cited by I. Skurada in *Handbook of Fiber Science and Technology*, Vol. IV, *Fiber Chemistry*, M. Lewin and E. M. Pearce (Editors), Marcel Dekker, New York, USA, 1985, p. 580.
23. A. Cohen. *Ann. Phys.*, 1898, **64**, 217.
24. A. J. P. Martin. *Proc. Phys. Soc.*, 1941, **53**, 186.
25. J. A. Medley. *Nature*, 1950, **166**, 524.
26. J. A. Medley. *Brit. J. Appl. Phys.*, 1953, Suppl. No. 2, S23.
27. J. A. Medley. *Brit. J. Appl. Phys.*, 1953, Suppl. No. 2, S28.
28. P. S. H. Henry, *Brit. J. Appl. Phys.*, 1953, Suppl. No. 2, S6.
29. P. S. H. Henry, *Sci. Prog.*, 1953, No. 164, 617.
30. P. S. H. Henry. *J. Text. Inst.*, 1957, **48**, P5.
31. F. A. Vick. *Brit. J. Appl. Phys.*, 1953, Suppl. No. 2, S1.
32. V. E. Gonsalves. *Text. Res. J.*, 1953, **23**, 711.
33. J. A. Medley. *Nature*, 1953, **171**, 1077.
34. G. W. Graham. *Nature*, 1951, **168**, 871.

24
Optical properties

24.1 Introduction

When light falls on a fibre, it may be partly transmitted, absorbed or reflected. Its behaviour in each of these three respects determines the visual appearance of the fibre, although the appearance of fibres in the mass may be considerably modified by the way in which particular arrangements influence the combination of effects in each fibre. The optical properties of fibres are also a useful source of information about their structure. In particular, the orientation of the polymer molecules can be estimated from differences in the refractive indices and in the absorption of light polarised in different directions relative to the fibre axis.

Rigorous analysis of the optical properties of fibres is a very complex subject and, whereas it is of great importance in studies of fibre structure, it does not justify a detailed discussion in a book primarily concerned with practical properties of fibres. The present chapter will be limited to a general account of the subject, particularly in its practical aspects.

24.2 Refraction

24.2.1 Refractive index and birefringence

The velocity with which light is transmitted varies with the medium through which it is passing. In isotropic materials, this property may be used to give the most fundamental definition of refractive index n namely, the ratio of the velocity of light in a vacuum to the velocity of light in the material. The study of this subject, and its consequence, is a well-known branch of physics. One particular result is that the direction of travel of light is refracted or bent on passing from one medium to another. This leads to an alternative definition: refractive index n = sine of angle of incidence/sine of angle of refraction.

The lower velocity of the waves means that the light waves are retarded on passing through a medium of high refractive index. If they are then combined with a beam that has passed through a different medium, various interference phenomena occur, and these may be utilised in the measurement of refractive index. In general, the refractive index of a material varies with the temperature and with the wavelength of

the light being transmitted. The usual standard conditions of measurement involve the use of monochromatic sodium light, with a wavelength of 589 nm, at 20 °C.

Light is composed of electromagnetic waves, and the change in velocity is associated with the electric polarisation that occurs under the influence of the electric field. The frequency of the waves is very high, so that only the polarisation of the electron distribution round the nuclei of atoms (i.e. the relative displacement of positive and negative charge) is important. Larger-scale effects, such as the rotation of permanent dipoles, cannot take place rapidly enough. The outer electrons, which are taking part in covalent bonds, are those affected, since electrons in the inner complete shells are not easily displaced: this is illustrated in Fig. 24.1. It is therefore possible to assign a polarisability to each chemical bond, although this is influenced to some extent by other atoms nearby. For example, there will be a small difference between the behaviour of a C—H bond in a —CH_2— group in a chain and that of a C—H bond in a terminal —CH_3 group. The polarisability will also vary with the direction of the electric field, as illustrated in Fig. 24.1(b) and (c): it is usually greatest when the field is directed along the line joining the atoms. However, in many simple materials, the molecules are arranged in all directions at random, so that the refractive index is the same in all directions and can be calculated from an appropriate summation of the polarisabilities of each bond in the molecule.

In anisotropic materials, such as textile fibres, the molecules are lined up in certain preferred directions, and the refractive index will therefore vary with the direction of the electric field, being usually greatest when the field is parallel to the axis of the molecules.

The direction of the electric field in an electromagnetic wave is known as the *vibration direction*. In ordinary light, there are vibrations in all directions at right

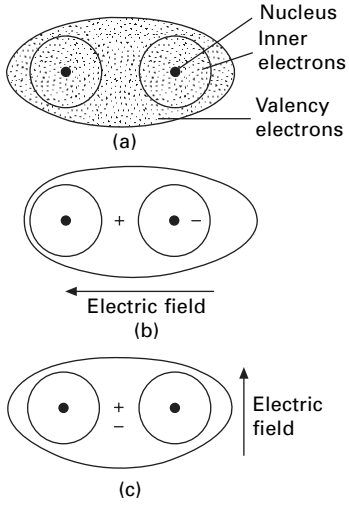

24.1 (a) Schematic representation of electron distribution around a pair of atoms linked by a covalent bond. (b) Distortion of distribution by an electronic field, acting along line between atoms, showing centres of positive and negative charge. (c) Effect of electric field perpendicular to line of atoms.

angles to the direction of transmission. When light is passed through an anisotropic material with uniaxial symmetry, the light splits up into two rays moving with different speeds corresponding to the components of the electric field parallel and perpendicular to the line of atoms: these are called the *ordinary* and *extraordinary* rays. They will be refracted differently and so may give rise to two separate images of an object viewed through the material. In appropriate circumstances, they may also interfere with one another because of the difference in retardation and cause the appearance of interference colours [1]. It is possible, by passing light through a Nicol prism or a sheet of polaroid, to polarise[1] the light so that it is vibrating in one direction only, the components in the perpendicular direction being completely eliminated. This enables one to study the variation in refractive index with the direction of vibration.

In general, an anisotropic material will have three principal refractive indices, but fibres are usually axially symmetrical so that the refractive indices perpendicular to the fibre axis are all the same. The principal refractive indices, shown in Fig. 24.2, are thus $n_{\parallel}$ for light polarised parallel to the fibre axis, and $n_{\perp}$ for light polarised perpendicular to it. In general, calculation of the refractive indices in other directions is complicated [2].

The refractive index of an isotropic fibre, n_{iso}, is given by the mean of the refractive indices of an oriented fibre in the three principal directions. That is:

$$n_{iso} = 1/3(n_{\parallel} + 2n_{\perp}) \tag{24.1}$$

The difference $(n_{\parallel} - n_{\perp})$ between the principal refractive indices is known as the *birefringence* of the fibre.

The above discussion refers to the intrinsic birefringence of a fibre due to the orientation of the crystal axes in the crystalline regions and of the individual molecules in the non-crystalline regions. However, Wiener [3] has shown that, if non-spherical particles which are smaller than the wavelength of light are embedded with a preferred orientation in a medium of different refractive index, then birefringence results. This happens even if each material is itself isotropic, and it is called form birefringence.

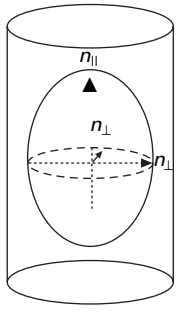

24.2 Principal refractive indices of a fibre.

[1]The word 'polarise' has more than one meaning. Polarisation of light is the limitation of the electric vibrations to one direction (the magnetic field is at right angles to this). Polarisation of atoms (or of a dielectric) implies the orientation or induction of dipoles (permanent or induced).

This type of birefringence may occur in fibres in which crystalline regions may be regarded as embedded in non-crystalline regions of different refractive index.

24.2.2 Measurement of refractive indices

If a fibre is immersed in a liquid of the same refractive index as itself, then its boundary ceases to be visible. By trial and error with a series of liquid mixtures of varying composition, the observation of this effect may be used as a means of measuring the refractive index of the fibre. It is, of course, necessary to use polarised light so that only one refractive index is concerned.

There are certain optical manifestations that may be used as aids in experiments of this sort. If the refractive indices of the fibre and the liquid are different, a bright line (the Becke line) can be seen at the boundary between them [4]. When the objective of the microscope is raised, this line moves towards the medium of higher refractive index. Another technique, which is simpler but less sensitive, is described by Heyn [5]. This makes use of the fact that a circular (or roughly lenticular) fibre acts rather like a convex lens and will focus a beam of light (Fig. 24.3). If parallel light comes from below, and the fibre has a higher refractive index than the immersion liquid, an image will form above the fibre. This may be observed as a bright band in the centre of the fibre when the microscope is focused above it. Conversely, if the refractive index of the fibre is less than that of the liquid, a virtual image will be formed below the fibre. The bright band will then be observed on lowering the microscope below the position where the fibre itself is in focus.

The above methods demand the rather tedious process of mounting the fibre in a large number of liquids. Frey-Wyssling [6] has adopted the technique of varying the wavelength of the light with which the fibre is observed in the liquid until the fibre outline disappears. On repetition of the process with a number of liquids, the dispersion curve (refractive index plotted against wavelength) can be found for the fibre. It is necessary to use a monochromator giving a high intensity of light.

Preston and Freeman [7] have used the same principle in a self-contained instrument. Rapid measurements can be made with this *fibre refractometer*. A prism and an associated optical system cast a spectrum onto a calibrated screen at one end of the

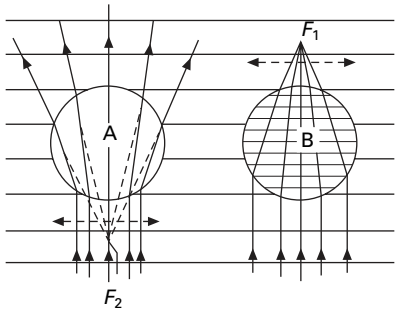

24.3 Formation of bright line in Heyn's method: (a) below the fibre at F_2 when the fibre refractive index is lower and (b) above the fibre at F_1 when it is higher.

apparatus. A glass cell, containing the appropriate liquid immersing a glass plate carrying the fibres, is placed in the path of the light dispersed by the prism. At the wavelength for which the refractive indices of liquid and fibres are equal, the light passes straight through and appears brightly on the screen. For other wavelengths it is scattered, and these parts of the spectrum do not appear focused on the calibrated screen. The wavelength of equal refractive indices can thus be read off directly on the scale. By variation of the temperature, equality of refractive indices can be achieved at various wavelengths, and, if suitable corrections are applied, the dispersion curve of the fibre may be found.

A somewhat similar modification has been introduced by de Vries [8]. If several ends of yarn, wound parallel to one another on a frame, are immersed in a liquid, they will act as a phase-grating and give a diffraction pattern if the refractive indices of fibre and liquid are different. If the refractive indices are the same, diffraction will not occur. In order to make use of this, de Vries observed the first-order diffraction spectrum through a spectrometer. Where the diffraction was absent, a dark band occurred on the spectrum observed in the spectrometer. Thus the wavelength at which the refractive indices were coincident could be found.

It should be noted that the various methods so far described may give different results because they measure the refractive indices of different parts of the fibre. It has been suggested that the Becke line gives the refractive index of the surface layers of the fibre, whereas Heyn's method of central illumination, Frey-Wyssling's method and Preston's refractometer give the refractive index of the bulk of the fibre. However, the problem is more complex than this, and detailed analysis is necessary before changes in refractive index across a fibre can be estimated. A full account of the subject has been given by Faust [9].

Variations in refractive index across a fibre are better investigated by interference techniques. In the interference microscope, differences in refractive index are transformed into colour changes if white light is used, or into dark and light fringes with monochromatic light. Heyn [10] has described how to use the method in the examination of fibre cross-sections.

Both double-beam and multiple-beam interference techniques have been used by Faust [11–14]. In the first method, Fig. 24.4(a), the light is split into two beams, one of which passes through the specimen, while the other bypasses it. The two are then combined and give an interference pattern. In the second method, Fig. 24.4(b), the specimen is placed between two partly silvered mirrors. A series of beams, which have passed through the specimen for a differing number of times, depending on the number of reflections, are transmitted by the system and combine to give the interference pattern.

There are various ways in which these techniques may be applied. For example, white light, with the interfering wavefronts parallel to one another, may be used. If this falls on a uniform specimen, such as a liquid in a cell, the condition for reinforcement of the interfering beams will be satisfied only at certain wavelengths. Consequently, if it is dispersed by a spectrometer, a series of bright and dark fringes at varying wavelengths will be observed. If a uniform fibre is immersed in the liquid, it will distort the fringes, as illustrated in Fig. 24.5(a). Where the fringe is in one straight

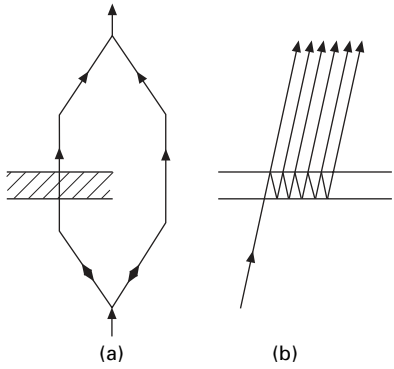

24.4 Schematic representation of (a) double-beam interferometry and (b) multiple-beam interferometry (the beam is inclined for the sake of clarity: it would actually be normal to the specimen, and the reflections would be back and forth along the same line).

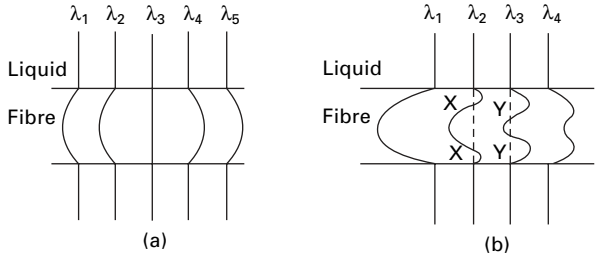

24.5 (a) Distortion of fringes with a uniform fibre. At wavelength λ_3, the indices are equal. (b) Distortion of fringes with a non-uniform fibre. The mean fibre indices are equal to the liquid indices at points X and Y for wavelengths λ_2 and λ_3, respectively.

line, the refractive indices of fibre and liquid must be equal. For other wavelengths, the fringe is curved owing to the varying thickness of fibre through which the light passes. An example of this is shown in Fig. 24.6(a), where the fringe for 519.2 nm is straight, which indicates that the indices are equal at this wavelength. However, if the fibre is not uniform in refractive index, the fringes will have a more complicated form, such as that shown in Fig. 24.5(b), and none will be straight. The mean refractive index at any position in the fibre can be found by observing the point at which the curved fringe in the fibre crosses the line of the fringes in the liquid. An example of this is illustrated in Fig. 24.6(b). If the dispersion of fibre and liquid is known, the variation in mean refractive index across the fibre, for a constant wavelength, can be calculated.

In two other methods, monochromatic light is used. With parallel light, the field in the liquid is uniform, and it is necessary to match the intensity in part of the fibre with that in the liquid. Alternatively, with the interfering wavefronts inclined to one another, wedge fringes are observed. Where these are in line with fibre and liquid, the indices are equal.

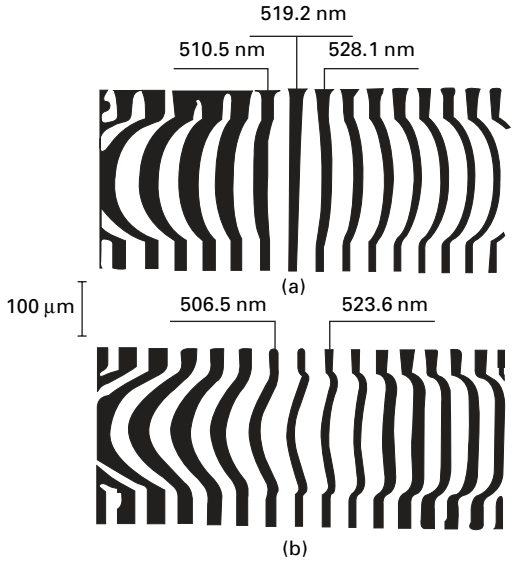

24.6 Interference fringes of varying wavelength, observed with an unstretched viscose rayon model filament immersed in a liquid of similar refractive index. Light vibration (a) parallel and (b) perpendicular to fibre axis. Wavelengths indicated in nm. After Faust [13].

24.2.3 Measurements of birefringence

The birefringence of a fibre is often determined by measuring the two principal refractive indices and subtracting one from the other. It can also be measured directly, however, by determining the retardation, or difference in optical path length, of the one principal ray relative to the other. Since the optical path length equals the product of the refractive index and the thickness of the specimen through which the light passes, it follows that retardation = $(N + \delta N)\lambda = (n_{\parallel} - n_{\perp})t$, where $N + \delta N$ is the number of wavelengths λ for which the light is retarded, and t is the thickness.

In order to find the retardation, it is necessary to measure both the whole number of wavelengths N and the fraction δN: the latter is usually easier to determine than the former.

When a fibre is viewed between crossed Nicol prisms, interference phenomena are observed. In the absence of a specimen, the field of view with crossed Nicols is dark because the polariser will pass only light polarised in one direction, and the analyser will pass only light polarised in a perpendicular direction. If a specimen is present with a principal direction parallel to the axis of either of the prisms, the field is still dark because the component of the light passed by the polariser will be transmitted without change by the specimen and stopped by the analyser. The four perpendicular directions for which this occurs are the extinction positions. If the specimen is at some other angle, however, for example with its principal direction at 45° to the axis of the prisms, the light passed by the polariser will be split by the specimen into two components X and Y, corresponding to the vibration directions of the light, and these will be transmitted at different speeds. When this light reaches the analyser, the

components of X and Y in the vibration direction passed by the analyser will be transmitted, so that the field will not, in general, appear dark, but, because of the differing velocity of transmission through the specimen, one component will be retarded relative to the other, and interference can occur. If there is a retardation of half a wavelength (or an odd multiple of half-wavelengths) the dark field between the crossed Nicols is changed into a bright one. Consequently, for a uniform circular fibre, viewed in monochromatic light, a series of light and dark bands will be seen parallel to the fibre axis, at thicknesses corresponding to retardations of odd and even numbers of half-wavelengths, respectively. In this way, the retardation, and hence the birefringence at various positions across the fibre, can be determined [15, 16].

When viewed in white light, only certain wavelengths satisfy the conditions for interference at a given place in the fibre, and thus interference colours are observed. By comparison with a standard colour chart, the retardation and birefringence can be deduced from these colours [4].

These two methods do not give results that are completely unambiguous. With the colours, the order of interference has to be estimated, and with monochromatic fringes it is not always easy to count close fringes, nor is it always certain that the retardation in a heterogeneous fibre is continuously increasing from fringe to fringe towards the centre. There are experimental dodges that can be used to overcome these difficulties, but a more accurate method of measuring birefringence is to use a compensator.

Compensators superimpose a known, but variable, retardation on that produced by the specimen. The simplest form is a calibrated quartz wedge, but there are other types, such as the Babinet and Berek compensators. If the retardation introduced by the compensator is equal and opposite to that introduced by the specimen, conditions are the same as if neither compensator nor specimen was present and so the field appears dark. The compensator can be adjusted until this condition is satisfied in order to determine the retardation at any point in the fibre, either by the use of white light or, if a more accurate setting is needed, by the use of monochromatic light. A full discussion of the difficulties involved in determining the retardation without ambiguity has been given by Faust and Marrinan [17].

Mortimer and Peguy [18] describe on-line measurement of birefringence.

24.2.4 Refractive index, density and swelling

Since the refractive index of a material is determined by an appropriate summation of the polarisabilities of the bonds present in each of its molecules, it is to be expected that the refractive index will increase as the number of molecules present increases, i.e. as the density increases. In many materials, the relation between the two is given by Gladstone and Dale's law, $(n - 1)/\rho$ = constant, where ρ = density.

This relation is an approximate form of the theoretical Lorentz–Lorenz expression. Hermans [19] has shown experimentally that the law applies to each of the refractive indices of cellulose fibres, although it does not necessarily apply to all anisotropic materials. If the average refractive index is used, the value of the constant is 0.3570.

A similar relation applies to mixtures. If v_m and n_m are the volume and refractive

indices, respectively, of a mixture, and $v_1, v_2, v_3 \ldots$ and $n_1, n_2, n_3 \ldots$ are the corresponding quantities for the individual components, the relation is:

$$v_m(n_m - 1) = v_1(n_1 - 1) + v_2(n_2 - 1) + v_3(n_3 - 1) + \ldots \quad (24.2)$$

For the two components cellulose and water, with the refractive index of water taken as 1.333, this expression reduces to:

$$v_r(n_r - 1) = v_0(n_0 - 1) + 0.333r \quad (24.3)$$

where v_0 is the volume of 1 gram of dry cellulose, v_r is the volume of the same specimen at a fractional regain r, and n_0 and n_r are the refractive indices of the dry and swollen cellulose, respectively.

Hermans [19] found that this relation, which is illustrated in Fig. 24.7, fitted the experimental results for cellulose. The rise in the curve at low regains corresponds to the increase in density that occurs as empty space is filled up (see Section 12.1.6).

Equation (24.3) applies to both the refractive indices $n_{\parallel}$ and $n_{\perp}$. If we substitute these in turn and subtract one equation from the other, we find how the birefringence varies with the swelling of the fibres:

$$v_r(n_{\parallel} - n_{\perp})r = v_0(n_{\parallel} - n_{\perp}) \quad (24.4)$$

This equation fits in with the experimental results up to regains of about 15%, and this is thought to indicate that the absorbed water is not preferentially oriented. If it were, it might be expected to add to the birefringence. Above 15% regain, the birefringence gradually becomes greater than the value given by equation (24.3). A possible explanation is that this is due to an increasing amount of form birefringence, arising from the arrangement of the crystalline regions within the non-crystalline regions. At low moisture contents, the differences in the refractive indices of the two regions are so small that the form birefringence would be negligible. At high moisture contents, however, since the moisture absorption takes place almost entirely in the non-crystalline regions, the differences are greater and may have an appreciable effect.

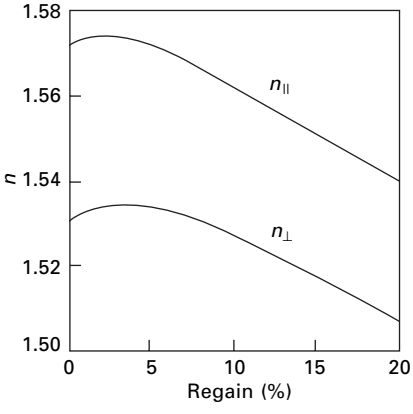

24.7 Variation of refractive indices of cellulose with regain. After Hermans [19].

24.2.5 Birefringence and orientation

We have seen that the difference in the refractive indices depends on the relation between the direction of polarisation of the light and the direction of alignment of the molecular chain. It is therefore to be expected that the birefringence will be greatest when the molecules are all lined up parallel to the fibre axis and that it will be zero when they are randomly directed.

Hermans [19] has defined an optical orientation factor f as the ratio of the birefringence of the fibre to that of an ideal fibre in which the molecules are perfectly oriented parallel to the fibre axis. Strictly, the expression should be corrected for differences in density by dividing each birefringence by the corresponding value of the density.

It is desirable to relate this factor to some geometrical measure of orientation, and Hermans has used the average angle of inclination of the molecules ϕ. This is defined as the angle of inclination in an imaginary fibre in which all the molecules are arranged at the same angle and which has the same birefringence as the actual fibre. He has shown that:

$$f = \frac{n_{\parallel} - n_{\perp}}{n'_{\parallel} - n'_{\perp}} \tag{24.5}$$

where $n'_{\parallel}$ and $n'_{\perp}$ refer to the ideally oriented fibre.

In a perfectly oriented fibre, $f = 1$ and $\phi = 0$. In an isotropic fibre, in which there is no birefringence, $f = 0$, so that $\sin^2 \phi = 2/3$ and ϕ is approximately 55°. It follows from equation (24.1) that:

$$n_{\text{iso}} = \frac{1}{3}(n_{\parallel} + 2n_{\perp}) = \frac{1}{3}(n'_{\parallel} + 2n'_{\perp}) \tag{24.6}$$

Consequently, the refractive indices vary with orientation in the way shown in Fig. 24.8. As an example, Table 24.1 gives some comparative values for cellulose fibres of varying degrees of orientation. As expected, the values of n_{iso} calculated from equation (24.6) are the same for differently oriented fibres, except for small differences in the third decimal place.

In cotton and other natural cellulose fibres, the birefringence is reduced, not because of random departure from a parallel orientation in the fibre, but because the molecules form a helix around the fibre axis. The index ellipsoid is thus placed at an angle to the fibre axis, as is shown in Fig. 24.9.

From measurements on highly oriented flax and ramie fibres, Meredith [20] deduced values of $n'_{\parallel} = 1.595$ and $n'_{\perp} = 1.531$; then, from measurements of $n_{\parallel}$, he calculated values of the spiral angle θ in 36 different cottons. Since the Becke-line method was used, he assumed that the values of refractive index and spiral angle were those of the outside of the fibre. Examples of his results are given in Table 24.2. The longer cottons have higher values of $n_{\parallel}$ and birefringence and a smaller helix angle.

In the above discussion, it has been tacitly assumed that there is no preferred orientation in the directions perpendicular to the fibre axis. This is not necessarily so. Even in a cylindrical fibre with axial symmetry, there may be a preferred orientation of crystallites in either of the two ways shown in Fig. 24.10. This will show up as birefringence when fibre cross-sections are observed, and between crossed polarisers

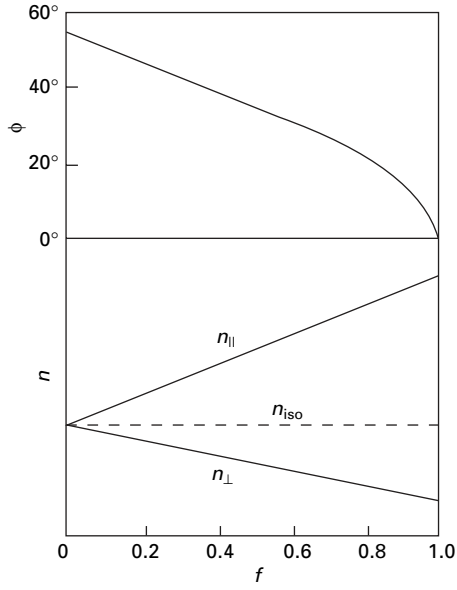

24.8 Variation of n and φ with f.

Table 24.1 Refractive indices, and related quantities, of cellulose fibres of varying degrees of orientation (reduced to a density of 1.52) (after Hermans [19])

Fibre	$n_{\|\|}$	$n_{\perp}$	$(n_{\|\|} - n_{\perp})$	f	ϕ	n_{iso}
Ramie	1.588	1.519	0.069	0.97	8°	1.542
Viscose rayon						
10% stretch	1.560	1.533	0.027	0.53	34°	1.542
80% stretch	1.568	1.531	0.037	0.74	25°	1.543
120% stretch	1.573	1.528	0.045	0.88	16°	1.542
Model filaments						
oriented	1.572	1.531	0.041	0.82	20°	1.544
isotropic	–	–	0	0	55°	1.544

interference colours will appear, except in the extinction directions of the polarisers. The resulting pattern will be a black cross on an illuminated ground. This is characteristic of radial orientation. In some fibres, it is apparent in the whole fibre; in others, such as some forms of regenerated cellulose, it appears only in the skin. In many viscose rayon fibres, the situation is somewhat more complex, as an original circular skin collapses to give a serrated outline. The type of orientation occurring is discussed in Section 1.5.2, and the polarisation effects observed are illustrated in Fig. 1.39.

24.2.6 Comparative values

Table 24.3 gives some values for the refractive indices of various textile fibres. All the values lie within the range 1.5 to 1.6, with the exception of the values for acetate, which fall below it, and the value of $n_{||}$ for *Terylene* polyester fibre, which is 1.725.

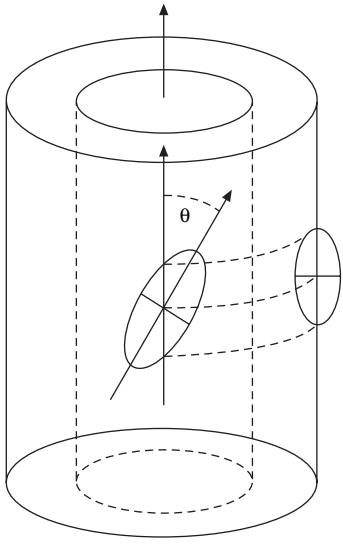

24.9 Index ellipsoid, and principal refractive indices, in a fibre with spiral orientation of chain molecules.

Table 24.2 Refractive indices, birefringence and spiral angle of cotton [20]

Cotton	Refractive indices			Birefringence of fibre ($n_{\|\|} - n_{\perp}$)	Spiral angle θ
	$n_{\|\|}$	$n_{\perp}$	n_{iso}		
St Vincent	1.581	1.530	1.556	0.052	27°
Montserrat	1.578	1.529	1.553	0.049	30°
Sakel	1.580	1.532	1.556	0.048	29°
Giza	1.579	1.530	1.554	0.049	29°
Tanguis	1.575	1.530	1.554	0.044	34°
Uganda	1.576	1.532	1.554	0.044	32°
Uppers	1.576	1.530	1.555	0.046	32°
Punjab-American 289F	1.577	1.530	1.553	0.047	31°
Brazilian	1.574	1.531	1.552	0.044	34°
Memphis	1.575	1.532	1.554	0.044	33°
Texas	1.575	1.532	1.554	0.044	33°
Oomras	1.574	1.532	1.552	0.043	34°
Bengals	1.574	1.531	1.551	0.043	34°

It is necessary to appreciate that the values given in Table 24.3 are only typical examples. Fibres are variable materials and their properties differ somewhat among the fibres in a sample, and to a greater extent between different varieties of the same type of fibre. The refractive index may also vary through a fibre cross-section. For example, Fig. 24.11 shows the variation across the fibre in the mean refractive indices of an unstretched viscose rayon model filament. The value of $n_{\|\|}$ is almost constant, but $n_{\perp}$ is a minimum at the centre. These values were calculated by Faust [13] from the interference fringes shown in Fig. 24.6.

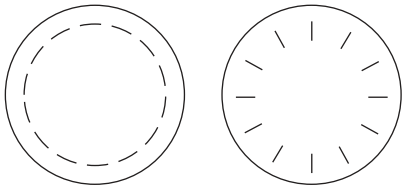

24.10 Two forms of orientation in the cross-section of a fibre with axial symmetry.

Table 24.3 Refractive indices of fibres

Fibre	$n_{\parallel}$	$n_{\perp}$	$(n_{\parallel} - n_{\perp})$	Ref.
Cotton	1.578	1.532	0.046	[21]
Ramie and flax	1.596	1.528	0.068	[21]
Viscose rayon	1.539	1.519	0.020	[21]
Secondary acetate	1.476	1.470	0.006	[22]
Triacetate	1.474	1.479	–0.005	[22]
Wool	1.553	1.542	0.010	[22]
Silk	1.591	1.538	0.053	[22]
Casein	1.542	1.542	0.000	[23]
Vicara (zein)	1.536	1.536	0.000	[4]
Nylon	1.582	1.519	0.063	[4]
Terylene polyester fibre	1.725	1.537	0.188	[24]
Orlon acrylic fibre	1.500	1.500	0.000	[4]
Acrilan acrylic fibre	1.520	1.524	–0.004	[4]
Polyethylene	1.556	1.512	0.044	[24]
Glass	1.547	1.547	0.000	[4]

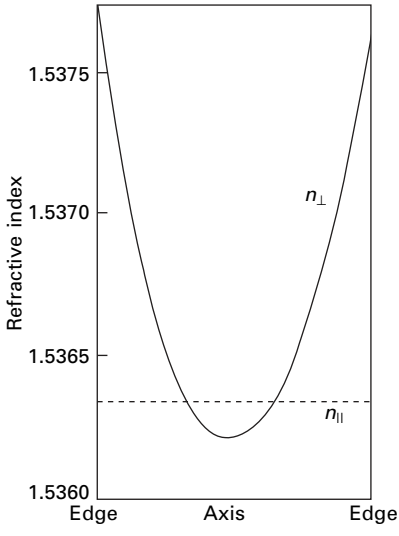

24.11 Variation in the mean refractive of an unstretched viscose rayon model filament [13].

The magnitude of the birefringence, which ranges from –0.005 for triacetate to 0.188 for polyester, depends on two factors: the degree of orientation of the molecules, as discussed in the last section, and the degree of asymmetry of the molecules themselves.

If all the atoms in a molecule are arranged in a straight chain (Fig. 24.12(a)), and if, as usually happens, the bond polarisabilities are greatest along the line joining the atoms, then, for the reasons discussed earlier, a high birefringence will be expected. However, the actual molecules in fibres do not have this form and their birefringence will be reduced for two reasons. Firstly, most main chains have a zigzag form (Fig. 24.12(b) but, provided that the bonds diverge from the main axis by less than about 55°, this still gives a positive birefringence. The coiling of the keratin molecule will have a similar effect in wool. Secondly, there will be side groups attached to the main chain, as in Fig. 24.12(c), and these will have the effect of providing atomic bonds at right angles to the main axis. This will increase the value of $n_\perp$ and reduce the birefringence. In triacetate and acrylic fibres, the side groups have a greater effect than the main chain, and the birefringence is negative.

A detailed study of the chemical structure of the molecules will account for the differences in the birefringence of perfectly oriented fibres. In polyester, the presence of a benzene ring in the main chain causes a great increase in the birefringence. If the orientation is not perfect, the birefringence will be reduced. This is shown up by the low values of birefringence of the regenerated protein fibres and by a comparison of the values for viscose rayon, cotton and ramie. Experiments on model viscose rayon filaments with varying degrees of orientation confirm this.

If the individual crystallites of a fibre could all be aligned in exactly the same orientation, with all their faces parallel, it would be possible to measure the three principal refractive indices of the polymer crystals. This cannot be done exactly, but Bunn and Garner [25] examined flattened nylon fibres, in which the crystallites are roughly parallel, and found the following refractive indices: 1.580 along axis of chain molecule, 1.565 normal to the flat sheets of the nylon crystal and 1.475 in the plane of the sheets and perpendicular to the fibre axis.

Gupta and Rao [26] report measurements of the birefringence of wool, which decreases with moisture regain and increases with stretching.

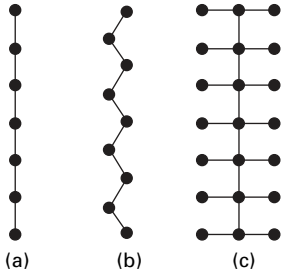

24.12 (a) Straight chain. (b) Zigzag chain. (c) Chain with side groups.

24.3 Absorption and dichroism

In addition to changing the velocity of light that is being transmitted, the interaction of electromagnetic waves and matter may also result in the absorption of the radiation. When this happens selectively in the visual region of the spectrum, it results in the materials appearing coloured when viewed in white light. Most textile fibres are either colourless or only slightly coloured in neutral shades. The absorption in the fibre itself is comparatively unimportant. In order to produce colours, the fibre must be dyed, but this subject is chiefly outside the range of this book. There is, however, one feature that is of physical interest. This is the variation in the absorption by the dye with the direction of polarisation of the light, the phenomenon known as *dichroism*, which may result in differences in the depth of shade or even in the actual colour. For this to happen, there are three requirements that must be satisfied. Firstly, the dye molecule must be asymmetrical, so that its absorption varies with the direction of the electric field exciting the characteristic vibrations. Secondly, the dye molecule must be absorbed into the fibre molecule in a particular direction, so that all the dye molecules make the same angle (or a limited range of angles) with the axis of the chain molecules. Thirdly, the chain molecules must be preferentially oriented.

When the first two conditions are satisfied, the magnitude of the dichroism may be used as a measure of the orientation of the molecules in the fibre.

The absorption of light in a material is given by Lambert's Law: $I = I_0\exp(-kd)$, where I is the intensity of light after passing for a distance d through a material with an absorption coefficient k, and I_0 is the intensity of the incident light. This may also be written:

$$\log \frac{I}{I_0} = -kd\,(\log \mathrm{e}) \tag{24.7}$$

For a material exhibiting dichroism, it is necessary to separate the light polarised parallel and perpendicular to the fibre axis, and we can substitute in equation (24.7) intensities $I_\parallel$, and $I_\perp$ and absorption coefficients $k_\parallel$ and $k_\perp$. Dividing one equation so obtained by the other, we get:

$$\frac{\log I_\parallel / I_0}{\log I_\perp / I_0} = \frac{k_\parallel}{k_\perp} = \phi \tag{24.8}$$

The quantity ϕ has been called the *dichroic* or *dichroitic ratio* or *constant* [27]. It has been found to be independent of the concentration of dye and may be used as a measure of orientation in the fibre. Values of the dichroic constant vary from unity in an isotropic material to infinity in a perfectly oriented fibre. Some typical values are given in Table 24.4.

Figure 24.13 illustrates one consequence of dichroism, namely that, when light passes through two dichroic fibres, there is a greater total absorption if they are crossed than there is if they are parallel. The reason is fairly obvious. If the fibres are crossed, the first fibre absorbs a large part of one component and the second fibre absorbs a large part of the perpendicular component, but if the fibres are parallel, the same component is absorbed by both fibres, and the perpendicular component is transmitted through both with little absorption.

Table 24.4 Dichroic constants for direct dyes on cellulose [27]

Material	Dichroic constant
Ramie	9
Viscose rayon	1.4–3.3
Cellophane	1.5

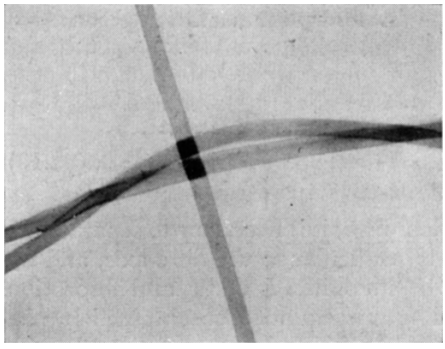

24.13 Exhibition of dichroism by cuprammonium rayon filaments dyed with chlorazol pink Y. The perpendicular crossed filaments appear darker than the nearly parallel ones. After Preston and Tsien [28].

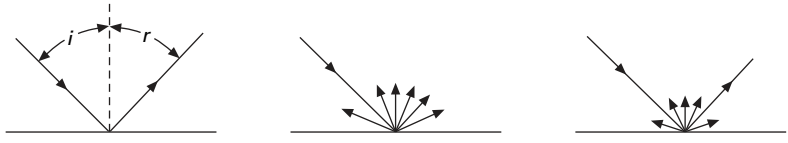

24.14 (a) Specular reflection. (b) Diffuse reflection. (c) Combination of specular and diffuse reflections After Buck and McCord [29].

24.4 Reflection and lustre

Lustre is an important aesthetic property of textile fabrics. If a beam of light falls on a surface, it may be reflected specularly, along the angle of reflection as in Fig. 24.14(a); diffusely, in varying intensity over a hemisphere as in Fig. 24.14(b); or in a combination of both as in Fig. 24.14(c). The reflection may vary with the angle of incidence and with the colour and polarisation of the light. The total visual appearance resulting from these reflections determines the lustre of the material. Lustre is thus easily observed subjectively but is extremely complex to characterise objectively.

This fact, together with the great importance of fibre arrangement in yarns or fabrics, has limited investigations of reflection and lustre from single fibres. Some general comments can, however, be made.

If a fibre behaved as a perfectly reflecting circular cylinder, it would reflect light as shown in Fig. 24.15. It is clear from this diagram that, if the light falls across the fibre, it is reflected at various angles, whereas if it falls along the fibre it is predominantly

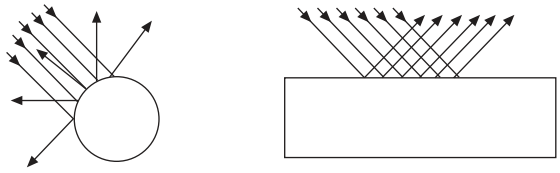

24.15 Reflection of light from a circular cylinder [29]: (a) axis normal to incident plane; (b) axis in incident plane.

Table 24.5 Lustre of a range of cottons

Type of cotton	Ratio of axes or cross-section, *a*/*b*	Lustre (arbitrary units)	Convolutions per cm, *c*
American FGM	3.07	5.7	31.3
Peruvian	2.62	6.7	30.0
Sakel S	2.37	7.1	29.8
St Kitts Sea Island	2.23	7.7	30.6
Surat	2.37	7.8	21.1
US 12, Sea Island	2.15	7.9	32.6
Abassi	2.21	8.0	30.9
Texas	2.22	8.1	29.3
Barbados Sea Island	2.17	8.2	31.4
Sakel CR	2.07	8.8	29.8
Egyptian, grown in Peru	2.11	9.0	30.5
Antigua Sea Island	1.91	10.7	29.9
Mercerised A	1.60	12.2	
B	1.64	12.9	
C	1.47	13.9	

reflected at a constant angle. This is a basic feature of textile lustre and shows the importance of causing the fibres to lie parallel to one another in a lustrous yarn or fabric.

Textile fibres depart from this ideal model in various ways. As was discussed in Section 3.3.3, finer fibres have a lustre which differs from that shown by coarse fibres. Irregularities on the surface of the fibre and in its cross-sectional shape will cause light to be reflected in various directions and will reduce the lustre. To secure the type of reflection shown in Fig. 24.15(b), it is essential that the fibre should be uniform along its length. For this reason, lustre is greatest in regular filaments, such as those of silk and the manufactured fibres.

Fibre shape is itself an important factor. The particular types of lustre associated with nylon, rayon and silk must be due partly to the influence on the pattern of light reflection of their respective circular, serrated and triangular shapes. In melt-spinning, shaped spinnerets can be used to make fibres with multilobal or other shapes, which become somewhat rounded as the molten material tends to a circular shape. This gives fibres with various lustre behaviour.

In cotton, Adderley [30] found a high degree of correlation between lustre and fibre ellipticity, as given by the ratio *a/b* between two axes taken, respectively, along

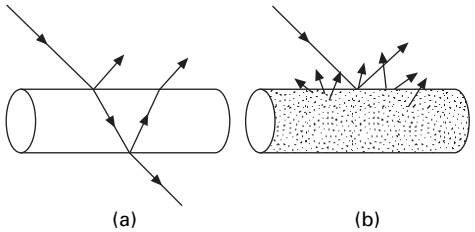

24.16 (a) Reflection, transmission and internal reflections in a fibre. (b) Scattering of transmitted light in delustred fibre [29].

the longest possible line through the fibre cross-section and perpendicular to this line at the mid-way position. Values for various types of cotton fibre are reported in Table 24.5, arranged in order of increasing lustre. Mercerisation, which swells the fibres and makes them rounder, increases the lustre of the fibres. Adderley found no connection between lustre and fibre length, linear density, diameter or the number of convolutions. However, in a theoretical investigation, Foster [31] found that for fibres with an elliptic cross-section, the lustre should be proportional to $[(a^2/b^2 + 1)/(a^2/b^2 - 1)]/ac$, where c is the number of convolutions per unit length. This relation gave reasonable agreement with the experimental results. The lustre of cotton is thus essentially due to a flat cross-section, of which the direction changes along the length of the fibre. If there were no convolutions, the light would be more regularly reflected, and the lustre would be different. The failure to observe any correlation between the number of convolutions and the lustre is due to the fact that the variations in c are not great, and their influence is marked by the much greater effect of the differences in a/b. It may, however, be noted that the Surat and US 12 cottons in Table 24.5, which show particularly high and low values of lustre for their values of a/b, are, respectively, the fibres with the lowest and highest values of c.

Not all the light falling on a fibre is reflected at its surface: much of it is transmitted through the fibre. Some of this transmitted light will be reflected from the internal surfaces, and will reinforce the light reflected from the first surface, as is shown in Fig. 24.16(a). If the fibre contains small particles (e.g. of titanium dioxide) or cavities, as in Fig. 24.16(b), these will scatter the transmitted light at varying angles and cause it to emerge as apparently diffuse reflection. This masks the specular reflection and may be used to delustre manufactured fibres.

It is a consequence of the effects of transmission and internal reflection that lustre will be influenced by variations in refractive index with the direction of polarisation of the light and with the position in the fibre. Once again, irregularities diminish lustre.

24.5 References

1. C. W. Bunn. *Chemical Crystallography*, Oxford University Press, London, 1946, Chapter III, p. 67 *et seq*.
2. N. H. Hartshorne and A. Stuart. *Crystals and the Polarizing Microscope*, Arnold, London, 2nd edition, 1950.

3. O. Wiener. *Abh. Sachs. Akad. d. Wiss. Math. Phys. Kl.*, 1912, **32**, 507, 604.
4. A. N. J. Heyn. *Text. Res. J.*, 1952, **22**, 513.
5. A. N. J. Heyn. *Text. Res. J.*, 1953, **23**, 246.
6. A. Frey-Wyssling. *Helv. Chim. Acta*, 1936, **19**, 900.
7. J. M. Preston and K. Freeman. *J. Text. Inst.*, 1943, **34**, T19.
8. H. de Vries. *Ann. Sci. Text. Belg.*, 1955, No. **4**, 286.
9. R. C. Faust. *Proc. Phys. Soc.*, 1951, **B68**, 1081.
10. A. N. J. Heyn. *Text. Res. J.*, 1957, **27**, 449.
11. R. C. Faust. *Proc. Phys. Soc.*, 1952, **B65**, 48.
12. R. C. Faust. *Proc. Phys. Soc.*, 1954, **B67**, 138.
13. R. C. Faust. *Quart. J. Micr. Sci.*, 1956, **97**, 569.
14. R. C. Faust. *Proc. Roy. Soc.*, 1952, **A211**, 240.
15. R. D. Andrews. *J. Appl. Phys.*, 1954, **25**, 1223.
16. R. D. Andrews and J. F. Rudd. *J. Appl. Phys.*, 1956, **27**, 990, 996.
17. R. C. Faust and H. J. Marrinan. *Brit. J. Appl. Phys.*, 1955, **6**, 351.
18. S. A. Mortimer and A. A. Peguy. *Textile Res. J.*, 1994, **64**, 544.
19. P. H. Hermans. *Physics and Chemistry of Cellulose Fibres*, Elsevier, Amsterdam, Netherlands, 1949, pp. 214 et seq.
20. R. Meredith. *J. Text. Inst.*, 1946, **37**, T205.
21. J. M. Preston. *Trans. Faraday Soc*., 1933, **29**, 65.
22. J. M. Preston. *Modern Textile Microscopy*, Emmott, London, 1933.
23. G. L. Roger and C. Maresh. *Text. Res. J.*, 1947, **17**, 477.
24. C. W. Bunn. In *Fibres from Synthetic Polymers*, R. Hill (Editor), Elsevier, Amsterdam, Netherlands, 1953, Chapter 10, p. 269.
25. C. W. Bunn and E. V. Garner. *Proc. Roy. Soc.*, 1947, **A189**, 39.
26. V. B. Gupta and D. R. Rao. *Textile Res. J.*, 1991, **61**, 510.
27. J. M. Preston. *J. Soc. Dyers Col.*, 1931, **47**, 312.
28. J. M. Preston and P. C. Tsien. *J. Soc. Dyers Col.*, 1946, **62**, 368.
29. G. S. Buck and F. A. McCord. *Text. Res. J.*, 1949, **19**, 715.
30. A. Adderley. *J. Text. Inst.*, 1924, **15**, T195.
31. G. A. R. Foster. *J. Text. Inst.*, 1927, **17**, T77.